Ministry of Education and Science of Ukraine
V. N. Karazin Kharkiv National University

Head of Department
of Molecular and Medical Biophysics
Dr. Sci., Professor
_____ Volodymyr BEREST
12.12.2024

MASTER`S DEGREE THESIS

INTERACTION OF CARBONIC ANHYDRASE WITH INHIBITORS

Scientific supervisor
Pavlína MALOY ŘEZÁČOVÁ
doc. RNDr., Ph.D.

Advisor
Volodymyr BEREST
Dr. Sci., Professor

Author
Anna MALIUKOVA
student of group RB-61,
specialty 105 Applied Physics and Nanomaterials

Kharkiv 2024

Acknowledgment

I would like to express my gratitude to the esteemed people from the structural biology group at the Institute of Organic Chemistry and Biochemistry in Prague, each of whom was kind enough to share their expertise with me. I am grateful for the assistance provided in developing the competencies essential for writing my thesis, for the fascinating exploration of carbonic anhydrase proteins, and for the motivation to work.

It is with the greatest appreciation that I express my gratitude to all those who have assisted me in my research. I am indebted to Pavlína Maloy Řezáčová, who has provided unwavering guidance and mentorship throughout my tenure in this esteemed group. I'd also like to thank Klára Pospíšilová for teaching me the Stopped Flow method and crystallization, Jiří Brynda for his invaluable assistance with the X-ray crystallography method, and to my esteemed and incredible scientific supervisor, I am truly grateful for all your support and its so grateful to have you by my side as I embark on my first adventure into the amazing world of science.

I would also like to acknowledge Mr. Roman Lesyk for providing the inhibitors that formed the basis of my thesis research into the interaction of these chemicals with proteins.

My biggest thanks goes to my family who always supports me and believes in me.

This project was supported by project Personalized Medicine – Diagnostics and Therapy, TN0100001 from Technology Agency of the Czech Republic, programme NCK.

ABSTRACT

Maliukova A. I. Interaction of carbonic anhydrase with inhibitors. Diploma theses for Master of Science Degree. V. N. Karazin Kharkiv National University, 2024. 67 p., 17 figures, 5 tables, 160 references.

CARBONIC ANHYDRASE, INHIBITOR, STRUCTURAL STUDY, STOPPED FLOW METHOD, X-RAY CRYSTALLOGRAPHY, TUMOR

The object of research: two proteins (carbonic anhydrase II and carbonic anhydrase IX) and three selected inhibitors.

Subject of research: the interaction of selected carbonic anhydrase inhibitors with specific carbonic anhydrase proteins.

The purpose of the work: investigation of inhibition properties.

Research methods: Stopped Flow method, vapour diffusion crystallisation by the hanging drop, X-ray crystallography.

Research results: X-ray crystallography studies have demonstrated that the selected inhibitors bind to the active sites of enzymes, forming strong hydrogen bonds with amino acid residues; kinetic studies have shown that the inhibitors have a high affinity for protein and are effective in reducing enzymatic activity. These results are relevant for further studies of these compounds.

Human carbonic anhydrases are metalloenzymes that are involved in a number of physiological processes within the body. Additionally, these enzymes are important in the pathogenesis of a multitude of diseases. Under physiological conditions, the expression of carbonic anhydrase IX (CA IX) is significantly less prevalent in comparison to the

fourteen alpha class isozymes. However, during hypoxia, this enzyme is highly overexpressed on the cell surface. For this reason, this enzyme represents an excellent target for the development of new therapies and diagnostic tools for tumors.Various anti-CAIX specific inhibitors are being developed.

The present study examines the interaction of three carbonic anhydrase inhibitors with two proteins, CA IX and CA II. Two of the three inhibitors are sulfonamides, and one of them is a thiazolidinedione. The inhibitory properties were investigated through the use of stopped-flow, crystallization, and X-ray diffraction techniques. Kinetic studies have demonstrated that the inhibitors possess a high binding affinity for proteinaceous substrates and are capable of significantly reducing enzymatic activity. X-ray crystallography studies have demonstrated that the selected inhibitors form strong hydrogen bonds with amino acid residues within the active sites of enzymes, thereby inhibiting enzyme function.

These findings can be a basis for further investigation of these compounds.

РЕФЕРАТ

Малюкова А. І. Взаємодія карбоангідрази з інгібіторами. Дипломна робота для магістерського ступеня. Харківський національний університет імені В. Н. Каразіна, 2024. 67 ст, 17 рис., 5 табл., 160 джерел.

КАРБОНАНГІДРАЗА, ІНГІБІТОР, СТРУКТУРНЕ ДОСЛВДЖЕННЯ, МЕТОД ЗУПИНЕНОГО ПОТОКУ, МЕТОД РЕНТГЕНІВСЬКОЇ КРИСТОЛОГРАФІЇ, ПУХЛИНА

Об'єкт дослідження: два білки (карбоангідраза II та карбоангідраза IX) та три відібрані інгібітори.

Предмет дослідження: взаємодія вибраних інгібіторів карбоангідрази зі специфічними білками карбоангідрази.

Мета дослідження: дослідження інгібувальних властивостей.

Методи дослідження: Метод зупиненого потоку, пародифузійна кристалізація висячою краплею, рентгенівська кристалографія.

Результати досліджень: Рентгеноструктурні дослідження показали, що відібрані інгібітори зв'язуються з активними центрами ферментів, утворюючи міцні водневі зв'язки з амінокислотними залишками; кінетичні дослідження показали, що інгібітори мають високу спорідненість до білка та ефективно знижують ферментативну активність. Ці результати є актуальними для подальших досліджень цих сполук.

Карбон ангідрази людини - це металоферменти, які беруть участь у низці фізіологічних процесів в організмі. Крім того, ці ферменти відіграють важливу роль

у патогенезі багатьох захворювань. У фізіологічних умовах експресія карбоангідрази IX (CA IX) значно менш поширена порівняно з чотирнадцятьма ізоферментами альфа-класу. Однак під час гіпоксії цей фермент сильно гіперекспресується на поверхні клітин. З цієї причини цей фермент є чудовою мішенню для розробки нових методів лікування та діагностики пухлин. Різноманітні специфічні інгібітори анти-CAIX в даний час розробляються.

У цьому дослідженні вивчається взаємодія трьох інгібіторів карбонової ангідрази з двома білками, CA IX і CA II. Двоє з трьох інгібіторів є сульфонамідами, а один з них - тіазолідиндіон. Дослідження властивостей інгібування було здійснено методами зупиненого потоку, кристалізації та рентгеностркуктурного аналізу. Кінетичні дослідження показали, що інгібітори мають високу спорідненість до білкових субстратів і здатні суттєво знижувати ферментативну активність. Рентгеноструктурні дослідження показали, що відібрані інгібітори утворюють міцні водневі зв'язки з амінокислотними залишками в активних центрах ферментів, тим самим пригнічуючи їхню функцію.

Ці результати можуть стати основою для подальших досліджень цих сполук.

LIST OF ABBREVIATIONS

CA(s)	Carbonic Anhydrase(s)
CA II	Carbonic Anhydrase II
CA IX	Carbonic Anhydrase IX
CAI	Carbonic Anhydrase inhibitor
CARP	Carbonic Anhydrase Related Protein
DMSO	Dimethyl Sulfoxide
HEPES	4-(2-hydroxyethyl)-1- piperazineethanesulfonic acid
HIF-1	Hypoxia-Inducible Factor-1
IC tail	Intracellular tail
Milli-Q water	water purified using a Millipore Milli-Q lab water system
PG domain	Proteoglycan-like domain
SP	Signaling Peptide
SF	Stopped Flow
TM	Transmembrane helix
Tris	Tris(hydrozymethyl)aminomethan
ZBG	Zinc-binding group
VHL	von-Hippel-Lindau-tumor suppressor
v/v	volume concentration

TABLE OF CONTENTS

INTRODUCTION AND AIMS

Carbonic anhydrase (CA) belongs to a large family of metalloenzymes. These proteins catalyze the reversible reaction of carbon dioxide hydration to bicarbonate ions and protons. This process plays a pivotal role in regulating the acid-base balance. Given their involvement in numerous biological processes, these enzymes are also also involved in various pathological conditions. This makes the inhibition of specific CA isoenzymes an important goal in the development of therapeutic agents for a wide range of diseases.

This work focuses on human carbonic anhydrase IX (CA IX) which is one of three membrane located CA isoforms. CAIX plays a significant role in cellular adaptation to low pH levels and is involved in the progression of cancer, as has been demonstrated. The protein expression on cell surface is induced in hypoxic conditions, thereby generating an acidic microenvironment through proton formation. This results in acidosis, which in turn fosters the survival and progression of cancer cells. In light of the aforementioned evidence, it is currently of great importance to create selective inhibitors of carbonic anhydrase IX and to investigate their inhibition properties. Carbonic anhydrase II (CA II) is not associated with cancer. It is widely distributed intracellular isoform that plays crucial physiological role. It has similar structure to CA IX, with the exception lacking PG and thansmembrane and intracellular domains that are unique to CA IX.

This study studies interaction of three carbonic anhydrase inhibitors with two proteins, CA IX and CA II. The objective is elucidating the inhibitory effects of these compounds in enzymatic assay and study the details of protein-inhibitor interactions by X-ray crystallogprphy.

To summarize:

The object of research: two proteins (carbonic anhydrase II and carbonic anhydrase IX) and three selected inhibitors.

Subject of research: the interaction of selected carbonic anhydrase inhibitors with specific carbonic anhydrase proteins.

The purpose of the work: investigation of inhibition properties.

Research methods: Stopped Flow method, vapour diffusion crystallisation by the hanging drop, X-ray crystallography.

Research results: X-ray crystallography studies have demonstrated that the selected inhibitors bind to the active sites of enzymes, forming strong hydrogen bonds with amino acid residues; kinetic studies have shown that the inhibitors have a high affinity for protein and are effective in reducing enzymatic activity. These results are relevant for further studies of these compounds.

1. STRUCTURE, FUNCTION AND INHIBITION OF CARBONIC ANHYDRASES

1.1 Carbonic Anhydrases

Carbonic anhydrases (CAs, EC 4.2.1.1) are metalloenzymes that catalyze the reversible hydration of carbon dioxide (CO_2) to bicarbonate anion (HCO_3^-) and proton (H^+) according to the following reaction:

$$CO_2 + H_2O \leftrightarrow HCO_3^- + H^+ \quad (1.1)$$

The primary function of this process is to maintain an optimal acid-base balance within the organism. Based on this, these proteins play a pivotal role in a number of crucial physiological processes: CO_2 and HCO^{3-} transport in respiration, bone resorption, gluconeogenesis, ureagenesis, lipogenesis, and cancerogenesis.

After identification of this enzyme in erythrocytes [139] it was found that it is present in large quantities in all tissues of mammals, plants, algae, and bacteria. CA has several different classes named by the Greek alphabet, which differ in their folded and oligomeric structures but all of them contain divalent metal ion in their active [144, 75]. Human carbonic anhydrase belongs to the alpha (α) class and has 15 isoenzymes that are structurally very similar and are involved in many important processes in the body, such as acid-base balance, electrolyte secretion, respiration, urogenesis, gluconeogenesis, and many others [144]. 12 of these 15 catalyze the reversible hydration of carbon dioxide via the above-mentioned reaction by Zinc ion in the active site and have a different range of catalyzed activity, while the other 3 (also called carbon anhydrase-related proteins (CARPs) do not contain Zinc (another metal), have different amino acid residues and therefore do

not perform catalyze [144]. Carbonic anhydrase isoforms are widespread within the human body, performing a diverse array of physiological functions. Figure 1 presents a schematic representation of the localization of human carbonic anhydrase isoforms.

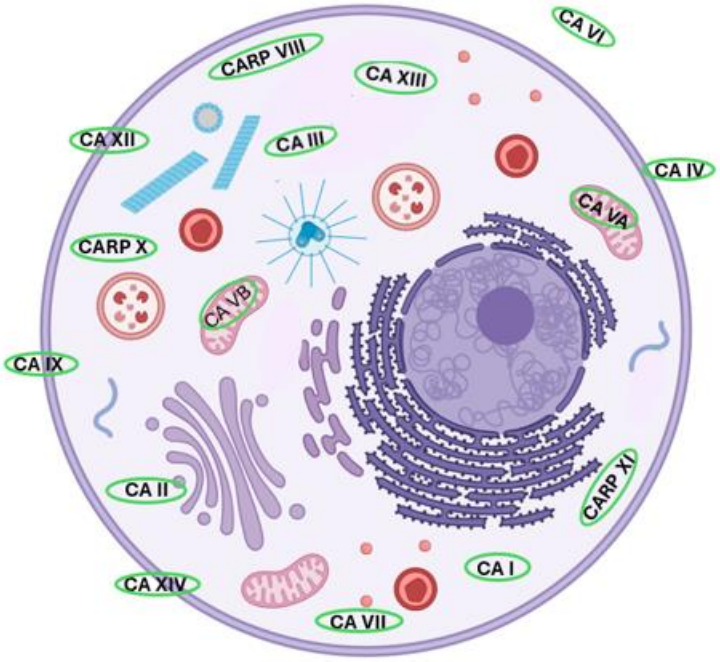

Figure 1.1. Schematic representation of the localization of human carbonic anhydrase isoforms: CARPs (CARP VIII, CARP X, CARP XI), CA I, CA II, CA III, CA VII, CA XIII are cytosolic proteins; CA VA, CA VB are mitochondrial proteins; CA VI is a secreted isoform; CA IV is a membrane protein with an anchor in the membrane; CA IX, CA XII, CA XIV are transmembrane proteins with inwardly directed sites. Proteins are schematically marked with green circles without taking into account their domain structure. The figure was created using the Biorender.com software. [161]

With the exception of CA VI, IX, and XII, the majority of CA isoforms are typically found in monomeric forms comprising seven right-handed α-helices and a twisted β-sheet formed by 10 β-strands (two parallel and eight antiparallel).

Carbonic anhydrase I is present in all body tissues. It exhibits moderate catalytic activity (CO_2 hydration). This cytosolic protein is predominantly present in significant amounts within erythrocytes, in addition to CA II, within the eyes or the gastrointestinal tract [158, 68, 83]. In individuals without health issues, the concentration of free CA I protein in the bloodstream is typically minimal. However, it can be markedly elevated in specific pathological contexts, such as prostate cancer [148], sepsis [61]. Additionally, CA I is implicated in the pathogenesis of retinal and cerebral edema [44].

CA II is the isoform most widely expressed and is involved in a multitude of processes, including bone resorption, respiration, and pH regulation. It displays considerable catalytic activity. The protein is distributed throughout a number of tissues, including the stomach, colon, kidney, erythrocytes, bone osteoclasts, lung, testis, and brain [98, 158, 8]. However, the activity of CA II has been linked to a number of diseases associated with blood and plasma, including hemolysis, disseminated intravascular coagulation, pulmonary hypertension, anemia, and stromal tumors of the gastrointestinal tract [47]. Moreover, the following conditions may be observed: renal tubular acidosis, osteopetrosis, cerebral calcification, glaucoma, edema, and epilepsy [98, 8].

It was shown that CA III performs an antioxidant function within cells that undergo significant oxidation, including adipose tissue, hepatocytes, and skeletal muscle fibers [99, 158]. The enzyme exhibits minimal catalytic activity. The CA III protein has been identified in the epididymis, skeletal muscle, and adipocytes [8, 98]. The activity of CA III is detected when the regulation is reduced in cases of liver damage [65, 24], acute coronary syndrome [130], or vasculitis [129]. However, typically it plays a more prominent role in the context of oxidative stress [98, 8, 87].

The carbonic anhydrase IV isoenzyme displays high catalytic activity (CO_2 hydration). CA IV is a membrane-bound CA that is anchored to the membrane via a glycosylphosphatidylinositol anchor. In normal tissue expression, the protein is found in the colon, cerebellum, kidney, lung, pancreas, brain capillaries, heart muscle, and eyes [98, 8,

158]. The protein has been linked to a number of pathological conditions, including retinitis pigmentosa, glaucoma, cerebrovascular accident [98, 8] and autoimmune pancreatitis [112].

Carbonic anhydrase V, which exists in two forms (VA and VB), is localized in the mitochondrial matrix. CA VA is located in the mitochondria of the heart, lungs, kidneys, spleen, and intestine, where it provides these organs with bicarbonates for glucogenesis and fatty acids for the synthesis of pyrimidine bases [142, 158]. In contrast, CA VB is found in skeletal and cardiac muscle, kidney, pancreas, gastrointestinal tract, brain, and spinal cord [106, 36, 134, 54]. The catalytic activity of VA is observed to be of a low-moderate level (low at pH 7.4, moderate at pH 8.2 or higher) while that of VB is found to be significantly higher. The importance of this enzyme in the human body was clarified by the emergence of CA V-deficiency syndrome in the absence of the enzyme [153]. Additionally, the CA VA and VB genes have been identified as potential biomarkers for the diagnosis of pancreatic cancer [10, 11].

The secretory form of carbonic anhydrase VI has been identified in various biological fluids and secretions, including milk, saliva, nasal secretions, and the epithelial lining of the digestive organs [158]. In study [120] demonstrated a correlation between loss of taste and decreased secretion of this protein. The degree of CO_2 hydration for this particular protein isoform is moderate. The diseases that are associated with this protein are caries and Sjögren's syndrome [14].

The function of CA VII (cytosolic CA) in the production of cerebrospinal fluid (CSF) in the central nervous system may be significant [54, 158, 126]. This protein, which belongs to the carbonic anhydrase family, exhibits high catalytic activity. Carbonic anhydrase VII may serve as a biomarker for epilepsy [98, 8], potentially influencing memory and learning processes [19, 140].

CARP VIII is notably expressed in the cerebellum, in nerve cell bodies, some astrocytes, as well as in the liver, lungs, heart, thymus, and kidneys [76, 158, 7, 149]. The

expression of this isoenzyme has been observed in such pathological contexts as melanoma-associated paraneoplastic degeneration of the cerebellum [12], non-small cell lung cancer [2], and colon cancer [111].

The carbonic anhydrase IX has moderate activity. It is one of two CA proteins that exist in a dimeric form. In accordance with standard biodistribution patterns, this protein is typically present in pancreatic ducts, gallbladder ducts, stomach and bile duct epithelium, cells lining the ventricles, and rapidly proliferating normal cells of the small intestine [159, 59, 50, 116]. It has been demonstrated that increased protein expression plays a significant role in the promotion of tumor survival in a multitude of different diseases, including non-small cell lung cancer, renal cell cancer, rectal cancer, pancreatic cancer, and breast cancer [71, 97, 46, 69, 53, 66, 29]. In hypoxic tumors, the CA IX protein is strongly activated, thereby assisting their survival (further discussion of this topic can be found in paragraphs 2.3) [116].

Carbon anhydrase-related protein X is localized to the cytoplasm of the myelin sheath [149, 158]. Furthermore, this protein has been demonstrated to play a role in the inhibition of the cytoplasm myelin sheath and the pathogenesis of acute disseminated encephalomyelitis in disease states [149, 96, 7].

The catalytic activity of CA XI is moderately high. It is expressed in the central nervous system, neurites, astrocytes, the neural body, and the choroid plexus [149]. Additionally, it is present in the spinal cord, pancreas, kidneys, liver, thyroid gland, and ovaries, albeit in much smaller quantities [7]. An elevated level of CA-RP XI expression in these tissues is associated with an increased risk of developing cancerous cells. For example, this may be the case of gliomas, astrocytomas, oligodendroglial tumors, and gastrointestinal stromal tumors [102, 62].

The CA XII protein, like CA IX, forms a dimeric structure, yet its structural composition differs from that of CA IX. Carbonic anhydrase XII exhibits a low level of carbon dioxide hydration. Similarly to CA IX, it is overexpressed in a significant proportion of

cancers. These include kidney cancer, brain cancer, colorectal cancer, lung cancer, breast cancer, cervical cancer, ovarian cancer, squamous cell cancer of the oesophagus, as well as pancreatitis, Sjögren's syndrome, cystic fibrosis-like diseases, rheumatism, and glaucoma [152, 115, 154, 156, 78, 52, 67, 123, 49, 113, 77, 86, 122, 125, 80, 158].

Furthermore, these isoforms (CA IX and CA XII) facilitate tumor adaptation to hypoxic microenvironments and promote metastasis [30].

Cytosolic carbonic anhydrase XIII is expressed in the tissues of the reproductive organs, where it plays a role in regulating pH and ensuring fertilization [34, 158]. It demonstrates moderate catalytic activity. In typical circumstances, this protein is observed in the colon and small intestines, as well as the testis, cervix, endometrial glands, and thymus [79]. In pathological conditions, CA XIII can be observed in colorectal tumors and Sjögren's syndrome [74, 119].

CA XIV is localized within the brain and the retina, where it is responsible for facilitating the removal of CO_2 from the neuronal retina and for modulating photoreceptor function [107]. Additionally, the enzyme is present in the kidneys, where it is instrumental in acidifying urine, as well as in the heart, skeletal muscles, and lungs [101, 63]. The enzyme in question exhibits a low degree of CO_2 hydration. In addition to it is expression in normal tissues, CA XIV has been demonstrated to be markedly overexpressed in a range of cancers, such as gliomas, liver and uterine cancers, melanomas [25, 45].

CA (in particular CA I and CA II) also represents an attractive model protein for a range of biochemical and biophysical studies, as previously outlined by study [72], offering a number of key advantages: it is monomeric, and stable, and can be easily mutated and purified with a high yield of *E.coli*; its structure was clearly defined; it simply catalyze a reaction; it has various simple assays to determine ligand binding; its structure does not change dramatically after the addition of a ligand; etc.

This thesis is focused on carbonic anhydrase IX however carbonic anhydrase II was also used. Given the widespread distribution of CA II within the body, this isoform was

employed in this study as a "off-target" protein in the development of CA IX inhibitors. This means that CAII isoforms should not be inhibited by the investigated compounds to avoid serious side-effects. In this study, CA II was also employed for structural studies of inhibitor binding in the conserved active site.

1.1.1 Active site

It is worth noting that CA II was the first member of the carbonic anhydrase family to be extensively researched by scientists due to its widespread distribution. As a result, it is regarded as a model for other members of this class. Thereby, in this paragraph about the active site of carbonic anhydrase, the numbering of all amino acid residues will be used according to the numbering of carbonic anhydrase II.

The human CAs active site is located at the bottom of a 15Å deep conical depression, one wall of which is formed by hydrophobic and the other by hydrophilic residues [37]. The catalytic ion Zn^{2+} is situated at the base of the cavity and is coordinated by a complex of three histidine residues, and a water molecule or hydroxide ion, depending on the phase of the CO_2-bicarbonate cycle (Fig.2.1 A).

In addition to histidine residues, the other two amino acid residues are also of significant importance. The Zn^{2+}-bound solvent molecule is involved in hydrogen bond interactions with another water molecule (the so-called deep water) and with the hydroxyl group of the conserved threonine residue (Thr199), which in turn is bridged to the carboxylate group of a conserved glutamic acid residue (Glu106) (Fig.2.1 B). These interactions enhance the nucleophilicity of the Zn^{2+} -bound water molecule and orient the CO_2 substrate in a favorable position for nucleophilic attack. For this reason, the Thr199-Glu106 residue, an important catalytic dyad for all α-CAs, is referred to as a gate-keeping residue [144].

The hydrophobic portion of the active site is responsible for binding to the hydrophobic CO_2 gas, while the hydrophilic portion is responsible for binding and releasing bicarbonate and proton (polar molecules) into the environment [37].

Although the core of the active site in α-CAs is highly conserved, there is variability in amino acid composition at its periphery [1]. These parts of the active site represent regiuns to be targeted by inhibitors to ensure selectivity to one isoform over others.

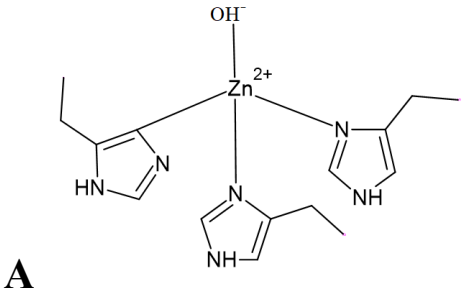

A

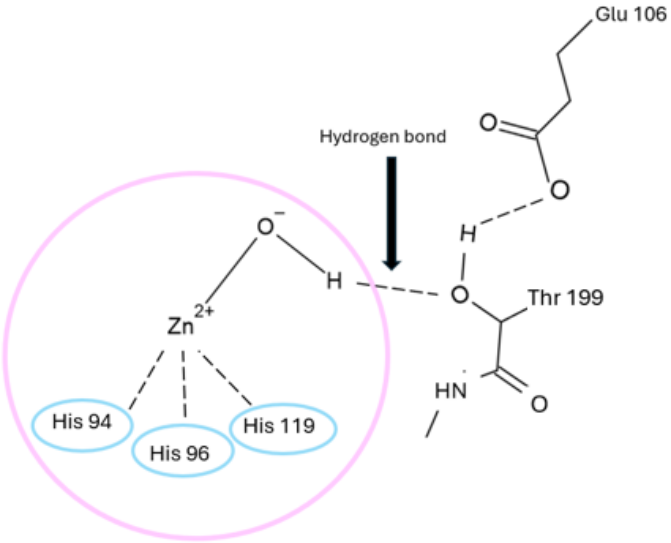

B

Figure 1.2. A) Schematic ofally shown Zn2+ ion that is tetrahedrally coordinated by three conserved histidines and a solvent molecule. B) The connection of the active site (indicated in the image with a purple circle) to Thr199-Glu106 residue. The CA II molecule is taken as a sample. The figure was initially created using the ChemSketch software and subsequently refined using the Microsoft PowerPoint application. [162]

1.1.2 Catalytic mechanism

The catalytic mechanism of CAs, also known as the ping-pong catalytic mechanism, comprises of two distinct steps. In the initial phase, the hydroxide ion bound to Zn^{2+} carries out a nucleophilic attack on the CO_2 molecule, resulting in the formation of a bicarbonate, which is then displaced by a water molecule. The second step realizes the transfer of the hydrogen ion from the water molecule either to the proton acceptor or the residue of the active site, thus restoring the bond between the hydroxide ion and the Zn^{2+} ion. The second reaction in the ping-pong mechanism, namely proton transfer, represents the rate-limiting step in the catalysis of CA enzymes [81, 27, 145]. The following two equations illustrate the catalytic mechanism:

$$1)\quad EZn^{2+} – OH^- + CO_2 \rightleftharpoons EZn^{2+} – HCO_3^- \rightleftharpoons EZn^{2+} – H_2O + HCO_3^- \qquad (1.2)$$

$$2)\quad EZn^{2+} – H_2O + B^* \rightleftharpoons EZn^{2+} – OH^- + BH^+ \qquad (1.3)$$

B* is a proton acceptor in the solution or a residue of the active site of the enzyme [37]. These two general steps of the ping-pong mechanism are reflected in the four stages presented in Figure 1.3, which illustrate the functioning of the enzyme.

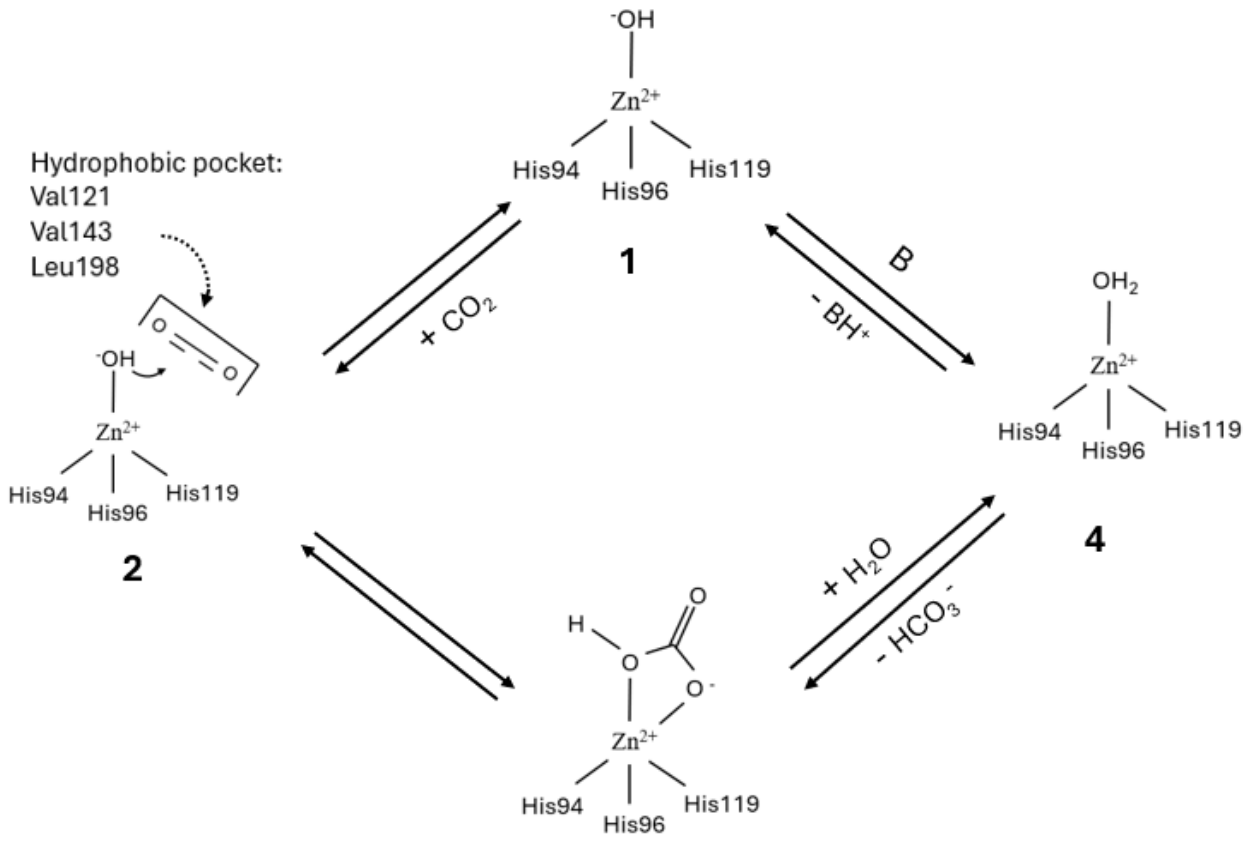

Figure 1.3. Catalytic mechanism of carbonic anhydrases on the example of CA II. 1) A metal hydroxide derivative, formed from water coordinated with a metal ion located at the bottom of the cavity of the active site of the enzyme, represents the catalytically active species. This exhibits a high degree of nucleophile reactivity (at neutral pH) on the CO_2 molecule that is bound in a hydrophobic pocket nearby. [37]. 2) The carbon dioxide substrate is bound in proximity to the Zinc (II) ion in a hydrophobic pocket**. 3)** In the third stage of the process, CO_2 (which is susceptible to nucleophilic attack) undergoes conversion into bicarbonate, which is linked to the Zn (II) ion in a bidentate manner. Given the labile nature of the bicarbonate-zinc binding, intermediate 3 is rapidly converted to 4 upon reaction with water, resulting in the release of bicarbonate into solution. 4) The formation of an acidic form of the enzyme with water coordinated to the metal ion (which is catalytically ineffective). The transfer of a hydrogen ion from a water molecule either to the proton acceptor or to the remainder of the active site forms the bond between the hydroxide ion and the Zn2+ ion, which contributes to the acquisition of the catalytic activity of the enzyme active site The figure was initially created using the ChemSketch software and subsequently refined in the Microsoft PowerPoint application. [162]

The His64 residue (CA II numbering) present is located at the entrance to the active site and, plays a crucial role in this context. Some studies have demonstrated that the residue His64 can exist in two conformations, namely in the middle (7.5 Å from Zn^{2+}) and outside (12 Å from Zn^{2+}), in an "in" and "out" state [9, 95, 108]. This indicates that CA proteins possess their own proton shuttle, whereby the histidine residue, having received a proton, transfers it to the solvent via a rotational mechanism. Nevertheless, an alternative viewpoint suggests that the proton transfer function of His64 is not determined by its rotation, but rather by the tautomerism of this residue [136].

Interestingly, the His residue is absent in CA III and CA V isoforms. The loss of the histidine residue may influence the relative decrease in the rate of catalysis due to the presence of larger, bulky residues that reduce the CO_2 binding area with the active site [38]. In carbonic anhydrase III, the residues Lys64, Ar 67, and Phe198 affect catalysis, rather than His64, Asn67, and Leu198 (CA II numbering), which influence the catalytic activity [41]. In CA V, a hydrophobic region is observed to prevail in the composition of the active site due to the presence of Tyr and Phe residues in place of Ala65 and His64 (in CA II). It is therefore postulated that these residues are not involved in the transfer of protons. Nevertheless, an alternative proton pathway involving residue Typ131 Lys132 is under consideration [16].

1.2 Carbonic Anhidrase II

Human carbonic anhydrase II (CAII) is a carbonic anhydrase widely distributed in the human body. It is predominantly present in erythrocytes, but is also found in almost all organs of the gastrointestinal tract, brain, kidneys, bones, and lungs. This cytoplasmic protein consists of 260 amino acid residues. The catalytic domain contains an active site

with a Zinc ion, which is coordinated by three histidines His94, His96, and His119. Hydrophobic residues are Val121, Val143, Leu198, Thr199, Val207, and Trp209 and hydrophilic residues are Tyr7, Asn62, His64 (which also present a transfer function described in paragraph 2.1), Asn67, Thr199, and Thr200. In addition to the histidine residue at position 64, which is located at the entrance to the active site, CA II also contains a cluster of histidine residues from the edge of the active site to the surface of the protein. This cluster (His4, His3, His10, His15 and His17) plays a crucial role in ensuring the active transfer of protons. This feature makes the CA II protein one of the most active known enzymes, given that the speed of this process approaches the limit of diffusion control [18]. Carbonic anhydrase II exists in a monomeric form with. Three-dimensional structure shown in Figure 4.

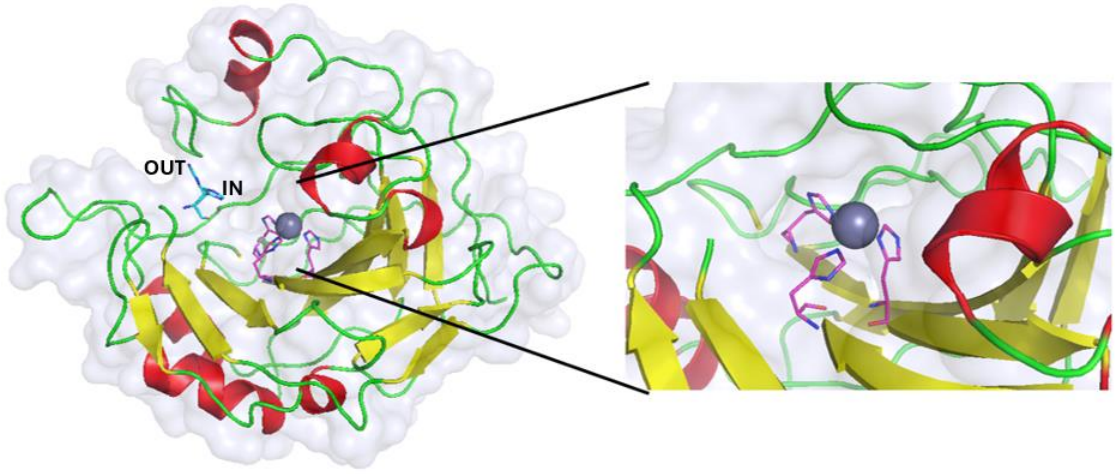

Figure 1.4. The three-dimensional structure of carbonic anhydrase CA II. The illustration on the left provides an overview of the enzyme's overall structure. It contains α-helices (colored red), folded β-sheet (yellow), and areas with irregular configurations (so-called loops, green). His 64 is shown in two conformations (blue color). The detail of the active site on the right figure shows Zn^{2+} (gray sphere), and its coordination with three histidine residues. Each figure was created in PyMOL software.

1.3 Carbonic Anhydrase IX

The isoform carbonic anhydrase IX (CA IX) was initially identified and designated the MN protein in studies conducted by [118], who also demonstrated a correlation between CA IX and tumor formation [160]. Nevertheless, further investigation revealed that this is a previously unidentified member of the human carbonic anhydrase class [114].

This protein under normal conditions in the body is mostly in the gastric mucosa, where it is involved in the formation of gastric fluid. Additionally, CA IX is present in small amounts in the mucosa of the bile ducts, the mucosa of the intestines, the epithelium of the pancreatic duct, and in the epithelial cells lining the body cavities. The physiological frequency of the CA IX protein is much lower than CA II, but the structure is much more complex.

The CAIX membrane protein consists of 459 amino acid residues. The sequence begins with 37 amino acid residues of the Signal Peptide (SP), which is cleaved during posttranslational modification. The extracellular N-terminal proteoglycan domain (PG), which is completely unique to the human CA IX isoform, comprises amino acid residues from 53 to 111. The catalytic domain (CA) is a common feature of all carbonic anhydrases, occurring between amino acid residues 137 and 391. PG domain as a CA domain is glycosylated [50]. Subsequently, a lengthy transmembrane (TM) segment is situated between amino acid residues 415 and 433, connected to a brief C-terminal intracellular region (IC), positioned between residues 433 and 459.

In the center of the active site is a Zinc ion, which is coordinated by three histidines, this time His226, His228, and His251. The hydrophobic region is defined by Leu91, Val121, Val131, Leu135, Leu141, Val143, Leu198, and Pro202, while the hydrophilic region is identified by Asn62, His64, Ser65, Gln67, Thr69, and Gln92. In the case of CA IX, the His200 residue is responsible for facilitating the transfer of a proton from the active site to the solvent.

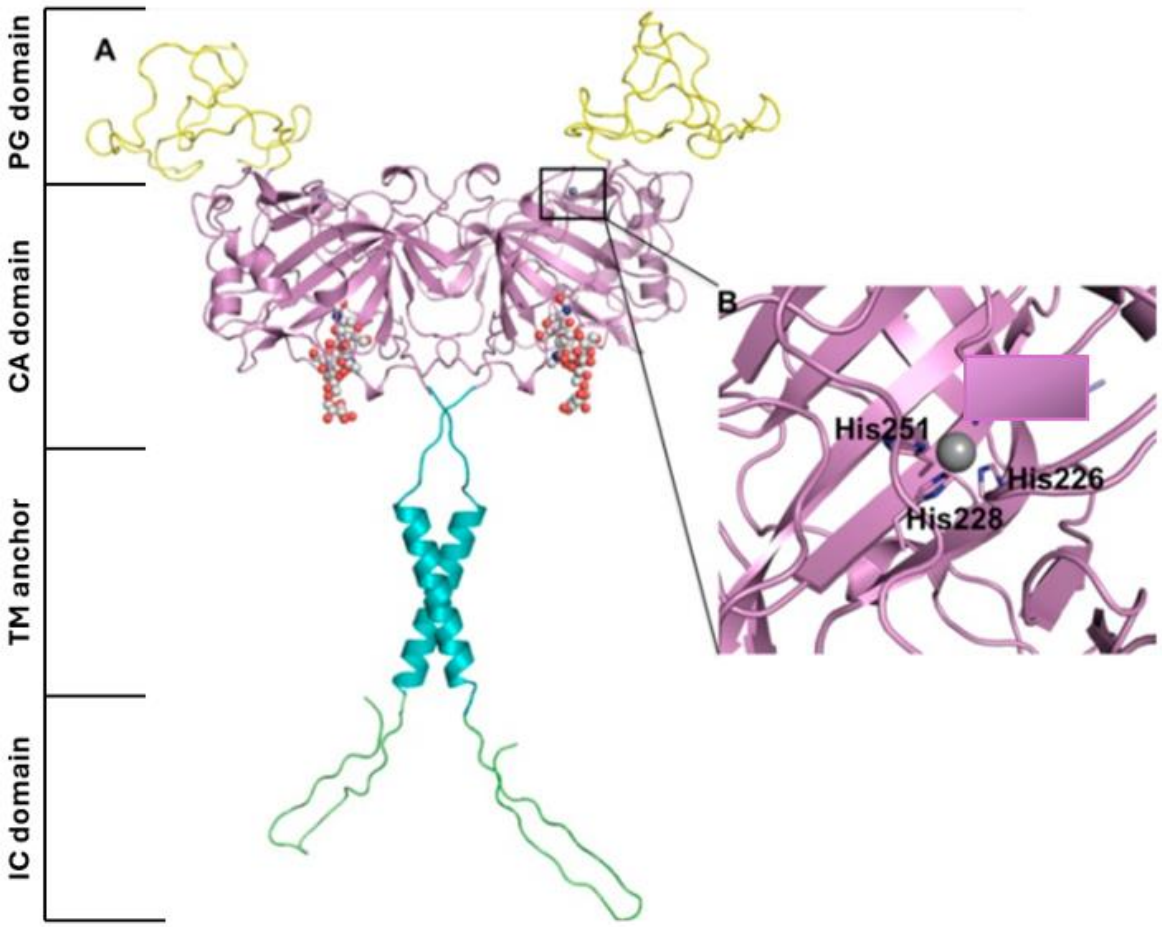

Figure 1.5. The structure of the dimer of CA IX (A). In the detail of the active site of the protein (B), three amino acid residues of histidine His 226, 228, and 251 coordinate the Zinc ion. The image was sourced from [85], with minor modifications for this particular study.

The enzyme forms a dimer (Fig. 1.5) through an intermolecular disulfide bond involving Cys137 as was shown in Hilvo et al, 2008. Additionally, N-linked and O-linked glycosylation sites are present at Asn309 and Thr78, respectively [50]. Two hydrogen bonds, involving the Arg137 side chain and the carbonyl oxygen of Ala127, and numerous Van der Waals interactions, contribute to the stabilization of the dimer, whose interface area extends over 1,590 $Å^2$ [5].

1.4 Carbonic Anhydrase IX in cancer

In the context of the disease, carbonic anhydrase IX is a tumor-specific, cell-surface glycoprotein that is induced by hypoxia. It plays a role in the adaptation of cells to low pH levels and has been linked to the progression of cancer. This occurs through its catalytic activity and/or non-catalytic functions [117].

Study [146] demonstrated that hypoxia leds to the activation of CA IX, which consequently resulted in an enhanced pH acidification. During hypoxia, the hypoxia-dependent factor HIF-1, which recognizes a specific sequence (TGCACGTA), so-called hypoxia-response element (HRE), in its promoter region, is activated, resulting in the expression of CA IX [155]. This is achieved through the formation of a heterodimeric complex consisting of α- and β-subunits. In normoxia, HIF-1 α forms a connection with pVHL (von Hippel-Lindau regulatory pathway), which results in the rapid degradation of the alpha subunit and prevents its combination with the beta subunit. In the event of an inadequate oxygen supply, the hydrogen bond between the proline residues of the subunit and pVHL is not formed. hereby the formation of a connection between the subunits of the factor (formation of HIF-1) which stimulates the transcription of the CA IX gene, thereby significantly enhancing its expression [85, 137, 117].

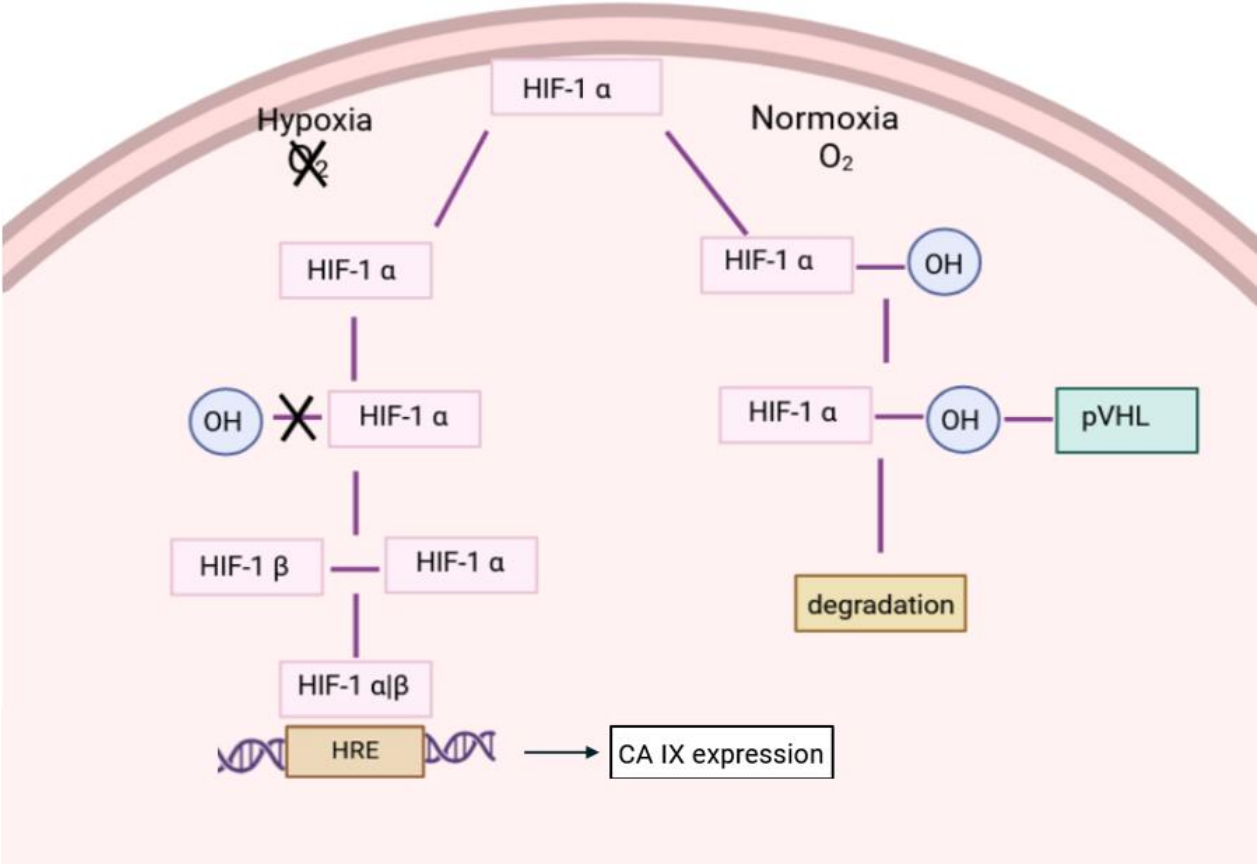

Figure 1.6. A schematic representation of the action of hypoxia-dependent factor HIF-1 in cell in normoxia and hypoxia, and its effect on the expression of CA IX in the latter case. The figure was initially created using the Biorender.com software.[161]

The protein creates an acidic microenvironment due to the formation of protons, which leads to acidosis, suppresses the immune response, contributes to the destruction of the extracellular matrix and the penetration of tumor cells into the surrounding environment, which in general promotes the survival and progression of cancer cells.

The manner in which CA IX can affect tumors is possible due to the activation of ion exchangers, pumps and transporters, such as sodium-dependent bicarbonate transporters (NBCe1, NBCn1 [100, 147]) and monocarboxylate transporters (MCT1, MCT4 [60]) that export lactate and protons (Fig. 1.7). The extracellular enzyme domain of the CA IX

protein, which catalyzes reaction 2.1, generates bicarbonate ions that enter the intracellular space with the assistance of NBCe1 and NBCn1. The resulting H^+ ions remain outside the cell, contributing to the acidification of the pericellular environment.

As for the PG domain, it is also involved in the tumorigenic activity of the CA IX protein. In the study [5] a sample was considered with and without the PG domain of CA. IX Their results demonstrate that the longer CA IX product, which contains the PG domain, acts as a superior catalyst for CO_2 hydration at more acidic pH values. The optimal pH level for this activity was found to be 6.49. This pH value is typically present in solid and hypoxic tumors, where we often observe elevated protein expression levels.

Discussing the relationship of CA IX to monocarboxylate transporters in this context, it should be noted, that lactate formed during glycolysis dissociates in aqueous solution into a lactate anion and a proton. The PG domain pumps protons from the cell by MCT, thereby establishing a proton gradient and increasing the negative charge on the inner cell surface relative to the outer cell surface. Concurrently, this process promotes the extrusion of lactate from the cell. Therefore, the PG-like domain functions through a non-catalytic process, in which the functions of the "antenna" are carried out [6].

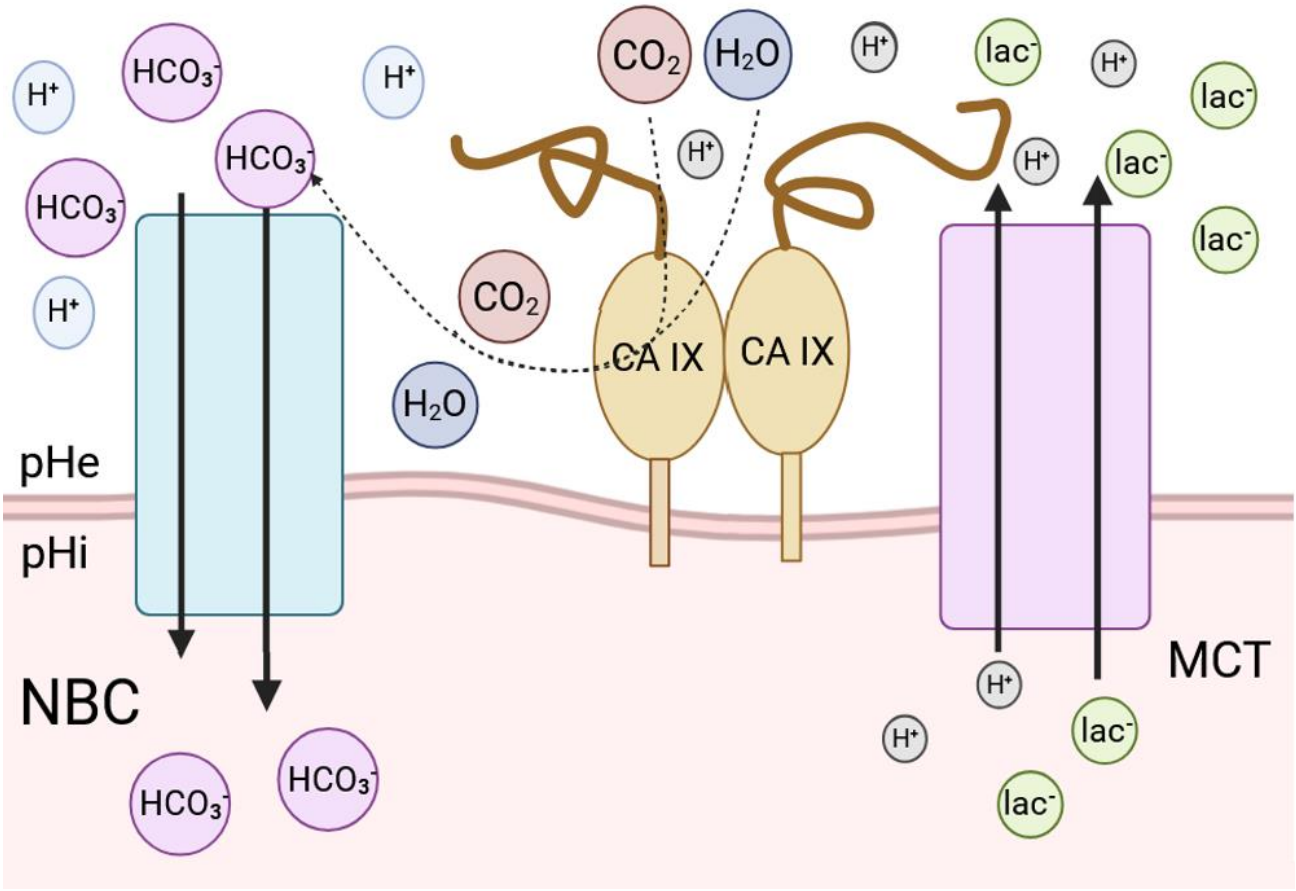

Figure 1.7. The schematic model demonstrates the function of CA IX in pH regulation in hypoxic cancer cells, working in conjunction with a sodium-dependent bicarbonate transporter (NBC) and monocarboxylate transporter (MCT). On the left, CA IX acts through its extracellular enzyme domain for bicarbonate transport, and on the right, lactate export is illustrated, which occurs through the non-catalytic action of the PG domain. The figure was created using the Biorender.com software. [161]

A growing tumor typically exhibits a number of key characteristics, including angiogenesis and invasion, increased proliferation, and the ability to adapt to microenvironmental stresses (such as hypoxia or acidosis). CA IX proteins regulate pH, producing an excess of acidic products, which enables tumors to adapt to metabolic changes in order to maintain their viability [117]. This supports the survival and proliferation of cancer cells.

As tumor growth progresses, this protein can even protect tumor tissues from adhesion or internal acidification. CA IX-induced extracellular acidosis can activate proteases, facilitating the breakdown of the extracellular matrix and enabling invasion. It can also promote angiogenesis and affect cell adhesion [117].

In this context, the inhibition of carbonic anhydrase IX represents a highly promising approach to controlling tumor formation and their vital metabolic activity.

1.5 Inhibition of Carbonic anhydrases

The inhibition of carbonic anhydrases, which represent established therapeutic targets, represents a promising avenue for the treatment of a wide range of diseases. Inhibitor binding to carbonic anhydrase can occur at either stage 1 or stage 4 of the catalytic mechanism (Fig. 1.8).

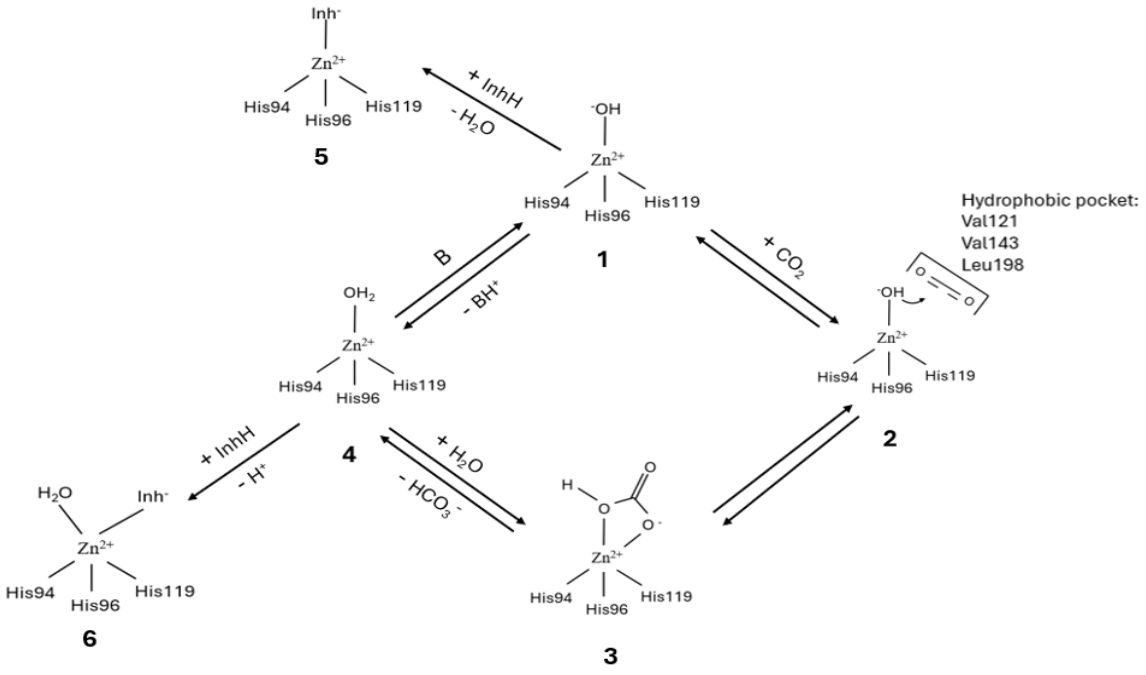

Figure 1.8. The inhibitory mechanisms are illustrated at the stages of the catalytic mechanism. The figure was initially created using the ChemSketch software and subsequently refined using the Microsoft PowerPoint application. [162]

The binding of α carbonic anhydrase can be classified into several categories [141]. The general structure of inhibitory molecules of various types of inhibition comprises a scaffold and a "tail" [4]. Given the conservative nature and similarity between the active site cavities of all α class CA enzymes, as previously discussed, it is the tail of molecules that can interact with variant residues in the middle of the active site and on the way towards the exit of the cavity that is of significant importance [132, 131, 17]. This method of synthesising inhibitors is known as “the tail approach”. The chemically distinct tails of inhibitor molecules can be modeled in order to exert influence over the physico-chemical properties of carbonic anhydrase inhibitors (CAI), which ultimately determine their biological activity [17, 131, 132].

The general mechanism of CA inhibition by Zinc binders (including sulfonamides (which will be discussed in paragraph 2.1), sulfamates, carboxylates, hydroxamates, and phosphonates) can be described as follows: in their deprotonated form as anions, these inhibitors bind to the divalent zinc ion by the zinc-binding group (ZBG) in the active site. Moreover, these inhibitors bind to the gate-keeping residues Thr199–Glu106 via the ZBG, thereby preventing the formation of a connection between these residues and the metal ion, as previously described in section 1.1.1. The scaffold of such compounds has the potential to occupy the hydrophilic/hydrophobic/both regions of the active site of the enzyme. The tails of the compounds are typically oriented towards the exit from the active site, where there are amino acid residues that vary considerably depending on the CA isoforms (Fig.1.9 A) [4, 33].

The initial compounds for which this novel binding mechanism by anchored to the zinc-coordinated water/hydroxide ion was documented were phenol and the polyamine spermine [109, 56]. In this category of inhibition mechanisms, compounds have an anchoring group (AG) attached to a scaffold that may also contain tails that interact with moieties of the active site in a manner analogous to that observed in the previously mentioned inhibitors (Fig.1.9 B). The anchoring group, which can be represented by a variety

of chemical functional groups, including phenolic, primary amine, ester and sulfonate, or just a simple sulfur atom, binds to zinc-coordinated water or hydroxide, as the name suggests, rather than directly to the zinc atom. [141, 22, 57, 13, 133, 58, 32, 23, 94, 150]. The scaffold, as the anchor group, can be a variety of structures. For example, research has already established that these can be aromatic, aliphatic, heterocyclic, or sugar types [124, 40, 128, 143, 88, 43]

This third mechanism of inhibition by occluding the entrance to the active site results in the binding of the inhibitory compound to the enzyme at the entrance to the cavity of the active site, which is the site that exhibits the greatest variability among different isoforms. This occurs via a sticky group (SG) attached to an aromatic, aliphatic, or heterocyclic framework. The tails of the compounds are capable of moving away from the active site due to the manner in which they bind within the outer cavity of the active site (Fig. 1.9 C). The first compound with such a described mechanism of action was isolated from the plant Leionema ellipticum and is a natural product of coumarins [92]. Following the discovery of this inhibition mechanism for coumarins [92, 91], it was shown to be an effective mechanism for other compounds such as substituted coumarins [151, 15, 135, 90, 89], 5- and 6-membered thiolactones and lactones [21].

Binding of inhibitor outside of the active site pockethe mechanism was identified during the crystallization of carbonic anhydrase II with 2-(benzylsulfonyl)-benzoic acid. The research team [31] observed that the electron density of the inhibitor was present in the adjacent binding pocket in close proximity to the active site. This represents a previously unobserved phenomenon among CA inhibitors. The inhibition of enzyme activity is caused by the blocking of the proton shuttle enzyme, His 64 residue, in its out conformation. This effectively prevents the transfer of a proton from the zinc-coordinated water molecule to the surrounding medium, thereby inhibiting the formation of zinc hydroxide. A schematic representation of this process is provided in Figure 1.9 D.

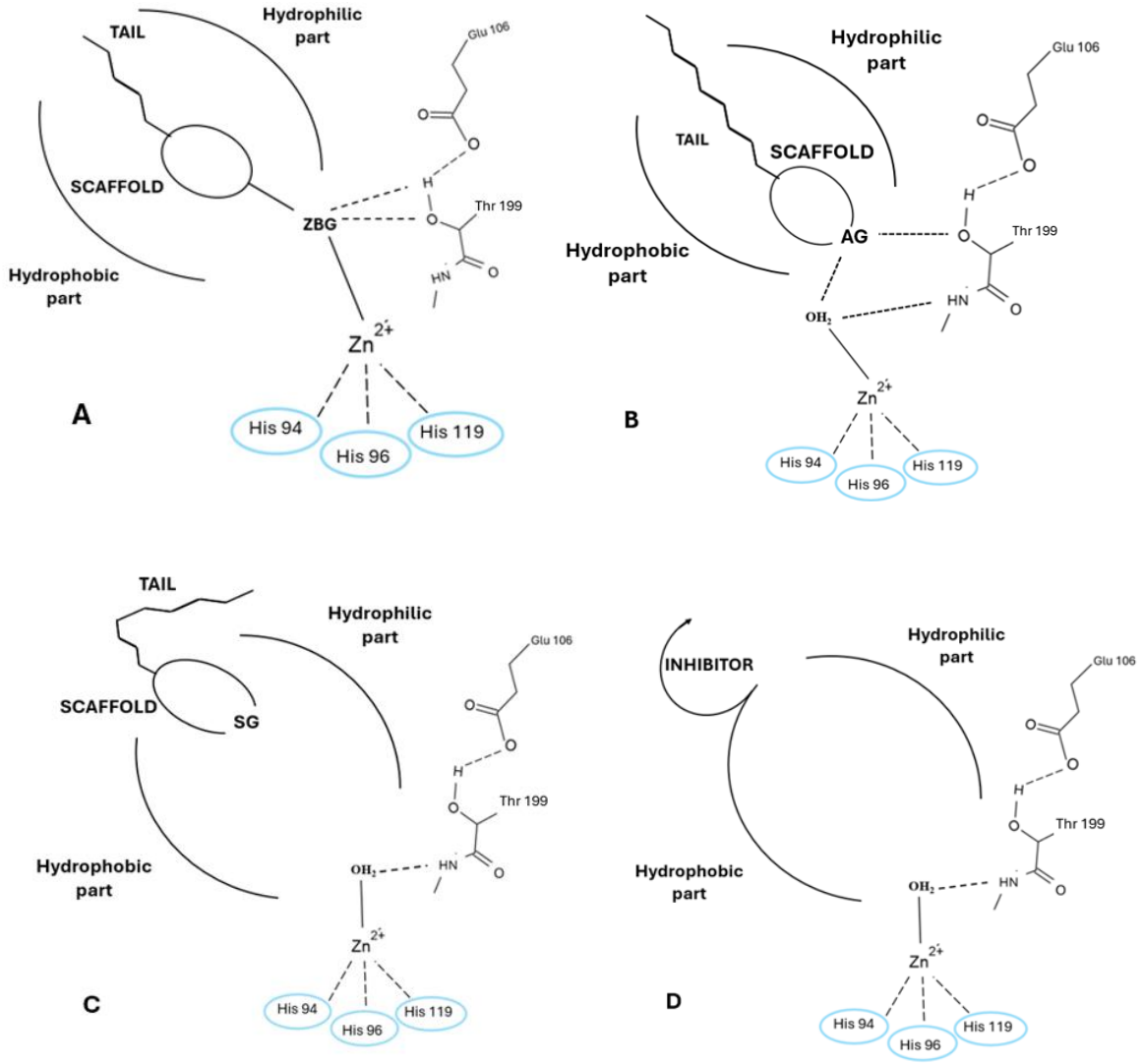

Figure 1.9**.** A) The schematic representation depicts the structure of a CAI molecule, which belongs to the class of compounds known as Zinc binders. B) The schematic image illustrates the structural configuration of the CAI molecule, which belongs to the class of CAIs that are anchored to the zinc-coordinated water/hydroxide ion. C) The schematic illustration depicts the inhibitory effect of CAI on enzyme activity through the occlusion of the entrance to the active site. D) The schematic representation depicts the mechanism of action of CAI, which binds to carbonic anhydrase outside the active site. The figures were initially created using the ChemSketch software and subsequently refined using the Microsoft PowerPoint application. [162]

2. MATERIALS AND METHODS FOR STUDYING THE INTERACTION OF COMPONENTS

2.1 Inhibitors

The conservation of the active site among proteins of the carbonic anhydrase class presents a significant challenge in the development of isoform-selective inhibitors. Consequently, inhibitors are subjected to continous improvement, modification, and synthesis of new compounds. In this study, three newly synthesized inhibitors are investigated. These inhibitors were taken from the research project of the laboratory where my work was performed, and they were synthesized by a collaboration laboratory of Professor R. Lesyk from Danylo Halytsky Lviv National Medical University, Ukraine.

Two of the inhibitors, designated CMP.1 and CMP.2 belong to the sulfonamide class of CAI.

Sulfonamides (general formula $R\text{-}SO_3NH_2$) and sulfamates represent the most significant class of CAIs. Their inhibitory effects on a diverse range of CAs, extending beyond the α-class enzymes, have been well documented [20, 138].

The main inhibitor compound (sulfonamide) forms the inhibitor head, followed by a linker attached to the compound body (aromatic ring), the latter part being the tail of the compound, which is a variable part of sulfonamide inhibitors and serves as a modification area. When CA is combined with an inhibitor, the sulfonamide head binds to the active site of Zn^{2+} carbonic anhydrase, and the different tail forms bond with other groups in the central domain, differently affecting the structure and function of metalloenzymes. The formation of two specific hydrogen bonds during the binding of sulfonamide ZBG ensures high selectivity for this bond with carbonic anhydrase while minimizing the likelihood of binding to other metalloenzymes [93].

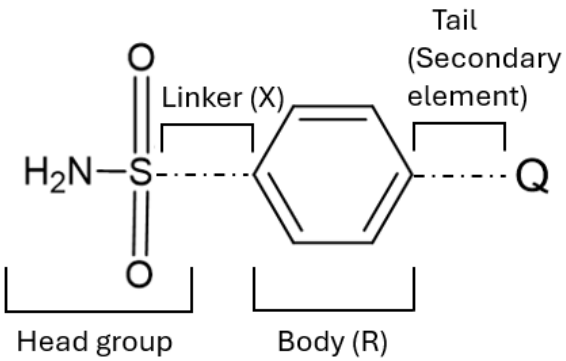

Figure 2.1. Schematically figure of sulfonamide inhibitor of CAs. The figure was initially created using the ChemSketch software and subsequently refined using the Microsoft PowerPoint application.[]

Sulfonamides and their derivatives (sulfamates, sulfamides) belong to the classic CAIs which have been explored for many decades. These are relatively small molecules that easily pass into the cavity of the active site and interact with its conserved residues and Zn^{2+}.

The third inhibitor (CMP.3) is a recently identified compound known as thiazolidinedione (general formula $RXNOS_2$) [28]. This inhibitor is constituted by a five-membered heterocyclic ring containing a sulfur atom, one nitrogen atom, and two carbonyl oxygens, which serve as the primary structural framework for the compound. In order to modify the pharmacological properties, a variety of substituents are added to the basic skeleton of thiazolidinediones, including aliphatic, aromatic, heterocyclic substituents, or polar groups.

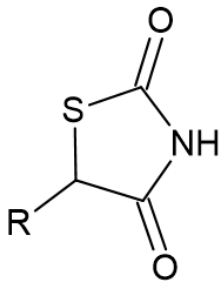

Figure 2.2. Schematically figure of thiazolidinedione inhibitor of CAs. The figure was initially created using the ChemSketch software. []

As previously stated, the objective of this study is to examine the mechanism of inhibition of the selected inhibitors (CMP.1, CMP.2, CMP.3) of the cancer-related protein CA IX in tumors, while ensuring the preservation of the activity of the most widely expressed carbonic anhydrase protein, CA II. Methods used to achive this objective are described in this paragraph below.

2.1.1 Inhibitor structure

Structural formula of the inhibitors used un this work cannot be disclosed as they are part of an ongoing research project aiming for scientific publication of patent application. However, for the sake of understanding further information and results, a brief description of the compounds will be provided here:

- In addition to the main ring, CMP.1 contains one five-membered heterocyclic ring and another six-membered homocyclic ring. In total, the compound contains thirty-six atoms.
- CMP.2 has a much shorter structure. Together with the main ring, one five-membered heterocyclic ring is presented here. The inhibitor's structural formula comprises twenty-three atoms.

- CMP.3 is represented by three rings, one of which constitutes the inhibitor basic skeleton, while the other two are six-membered homocyclic rings. The structure of the third compound contains thirty-two atoms.

Table 2.1. A graphic representation of the inhibitors presented in this work.

Name	Structure
CMP.1	Confidential 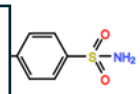
CMP.2	Confidential 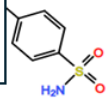
CMP.3	Confidential 

2.2 Chemicals

4-(2-hydroxyethyl)-1-piperazineethanesulfonic acid (HEPES)	Sigma-Aldrich, USA
Phenol red	Lacema, Czech Republic
Sodium citrate tribasic dihydrate ($C_6H_5Na_3O_7$ x 2 H_2O)	Sigma-Aldrich, USA
Sulfuric acid (H_2SO_4)	Sigma-Aldrich, USA
Tris(hydrozymethyl)aminomethan (TRIS)	Merck, German
Triethylamine (TEA)	Sigma-Aldrich, USA

2.3 Solutions and buffers

Buffer of CAs for Stopped Flow	
4%	Phenol red
200 mM	Na_2SO_4
500 mM	HEPES, pH 7.5

Solution for crystallization	
1.6 M	$C_6H_5Na_3O_7$ x 2 H_2O
50mM	TRIS-H_2SO_4, pH 7.8

2.4 Instruments

optical microscopes	Olympus SZX10, Japan
photo camera	Olympus E-620, Japan
pH meter	GMH 3430 Griesinger Electronic, Germany
	Orion™ 9110DJWP Double Junction pH Electrode, Thermo Scientific, USA
Stopped-Flow machine	Mixer 4000 (SFM 4000), BioLogic SAS, France
	Spectrophotometer, Bio-Logic SAS, France
X-ray Diffraction Station	MicroMax™-007 HF Microfocus,
	VariMax™ VHF Confocal Optical System, RIGAKU, Japan
	PILATUS 300K crystallography from Dectris, Switzerland
	Cryostream 600 series, Oxford Cryosystems Ltd, UK
Heating magnetic stirrer	HSC7, VELP Scientific, Inc, USA
Laboratory balances	IoT-Line Compact Laboratory Balance PCB 1000-2, © 2024 KERN & SOHN GmbH, Germany

2.5 Other material

crystallization utensils	15-Well Tools (20), Qiagen, Germany
	15-Well Tools (20), Qiagen, Germany
	X-Seal crystallization supports, Qiagen, Gemany
	MicroMounts™, MiTeGen, USA
other glassware	Bottle with screw cap PP, clear, 0.1-1 L, DURAN®, P-LAB, Czech Republic
centrifuges	Benchmark Scientific MyFuge™ C1008-G, USA
	Hettich Zentrifugen Mikro 200R, Germany

2.6 Software and databases

CCP4 software package (MOLREP, REFMAC5, COOT, AceDRG)

MolProbity 4.5.2

PyMOL Molecular Graphics System, Version 3.0 Schrödinger, LLC

2.7 Enzyme kinetics

In the course of my experiments, CA II and CA IX (and CA IX mimic) proteins were used. Both protein were produced by heterologous expression in *E. coli* and purified the structural biology group at the Institute of Organic Chemistry and Biochemistry using a described protocol.

The CA IX mimic is a variant of the CA II protein that contains six amino acid substitutions: A65S, N67Q, E69T, I91L, F130V, K169A, and L203A was used as a CAIX mimic for X-ray studies. The modifications were made to the active site of CA II to re-semble CA IX by mutating residues in the active site template of CA II to residues unique

to CA IX. This variant maintains the advantageous crystallization characteristics of CA II and is often utilized in structural investigations [48, 121].

Table 2.2. General information of the proteins that are used in stopped flow research.

Name	Concentration (mg/ml)	System	Buffer		
CA II	0.8	*E.coli*	50 mM	Tris base - H_2SO_4	pH 7.8
CA IX	1.2	*E.coli*	20 Mm 100 mM	TEA NaCl	pH 7.3

Table 2.3. General information of the proteins that are used in crystallization technique.

Name	Concentration (mg/ml)	System	Buffer		
CA II	25	*E.coli*	50 mM	Tris base - H_2SO_4	pH 7.8
CA IX mimic	21.56	*E.coli*	20 mM 100 mM	Tris-HCl NaCl	pH 7.5

2.7.1 Stopped Flow method

All enzymatic assays reported here were obtained using a Stopped-Flow Mixing system (SFM 4000 Stopped-flow Bio-Logic, France) connected to a spectrophotometer (Bio-Logic, France) based on the methodology described by Khalifah [64]. The assay buffer consisted of 0.2 mM phenol red (a pH indicator employed at the 557 nm, because of Ne-Hg lamp usega), 40 mM Na_2SO_4 (Ensures uninterrupted support of ionic strength),

and 40 mM HEPES at a pH of 7.5 (as a buffer). In order to obtain a substrate, CO_2 solution, gaseous carbon dioxide was introduced into a Milli-Q water sample over a period of 45 minutes. A second flask of Milli-Q water was subjected to a vacuum for a period of 45 minutes in order to remove any other gases that may have been present. The CA II and CA IX enzymes were maintained on ice until the commencement of the experiments, while the buffer solution was kept at a temperature of 25°C. In the inhibition assay solutions were loaded into temperated syringes S1(degassed Milli-Q water), S2 (CO_2), and S3 (enzyme-inhibitor mixture). The reaction is started by mixing of all componets in mixer on the way to measuring cuvete. The ratio of volumes was 1:1:2.

The final CO_2 concentration in the reaction mixture was predominantly 8.5 mM, with the enzyme concentrations of 4.1-7 nM for CA II and 18-26 nM for CA IX. The inhibitor stock solution (10 mM) was dissolved in dimethyl sulfoxide (DMSO) in a concentration range from 10 mM to 0.01 mM. The enzyme and inhibitor mixture was pre-incubated for a period of five minutes at a temperature of 25°C prior to injection into syringe S3. The rates of the CA-catalysed CO_2 hydration reaction were monitored over a period of 30 seconds at a temperature of 25°C. The experiment commenced with the measurement of the blank, which entailed gauging the speed of the pH level change in the buffer without the addition of catalysing protein and inhibitor over a period of 30 seconds. Subsequently, the mean value of the measured blank was subtracted from the total observed speed of all measurements. This subtraction is due to the spontaneous conversion of CO_2 to bicarbonate (the uncatalysed 8.5 mM CO_2 is being completely converted to bicarbonate in approximately 30 seconds under the aforementioned conditions). All the measurements were performed in triplicate to get a robust results.

The apparent K_i values were determined from dose-response curves recorded for a minimum of five distinct concentrations of the test compound. This was achieved through the utilisation of the nonlinear least squares method to fit the Williams-Morrison equation [103]:

$$v_I = v_0 \frac{[E] - [I] - K_i^{app} + \sqrt{([E] - [I] - K_i^{app})^2 - 4[E]K_i^{app}}}{2[E]} \quad (2.4)$$

v_I represents the initial velocity of an inhibited reaction, whereas v_0 denotes the velocity of a non-inhibited reaction at its inception. $[E]$ signifies the concentration of an active enzyme, while $[I]$ represents the concentration of an inhibitor. K_i^{app} is the apparent constant of inhibition.

A dose-response curve is a graphical representation of the dependence of the reaction rate on the concentrations of the inhibitor. The shape of these graphs and their associated parameters can be employed in the calculation of the value of K_i. An exponential fit of the reaction rate over time was used to determine the initial reaction rate.

In light of the presence of CO_2 gas as a substrate and the competitive inhibitors in reaction, it is necessary to calculate the actual K_i values through the Cheng-Prusoff equation [157],

$$K_i = \frac{K_i^{app}}{1+[S]/K_m} \quad (2.5)$$

with the K_m value of 9.3 mM applied for CA II [56] and 7.5 mM for CA IX [50] in the calculations, S is substrate concentration.

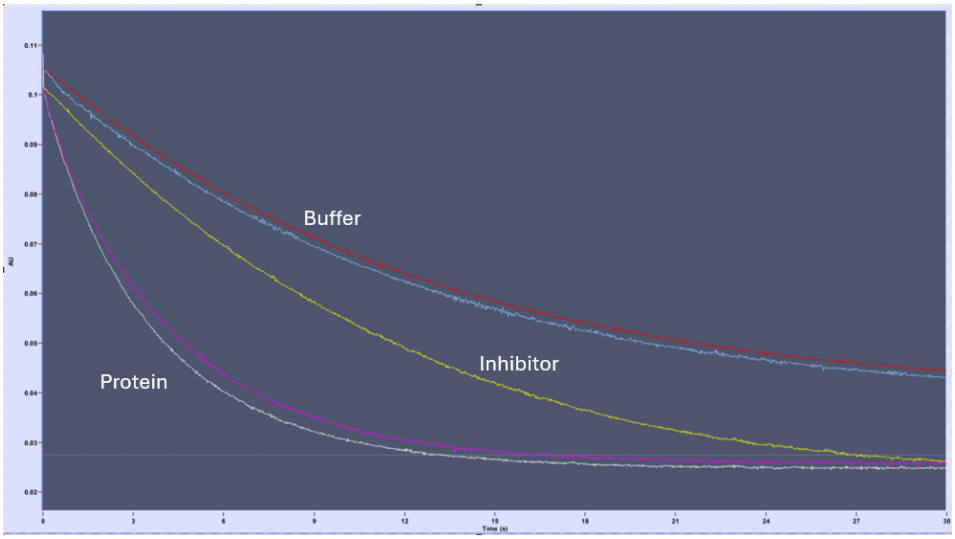

Figure 2.3. Absorbance curves for inhibition. The following curves represent the change in absorbance over time, as reported by the phenol red pH indicator, as a consequence of CO_2 hydration obtained using BioKine software. Under the buffer here is the buffer for measuring the reaction. Protein means Stopped Flow buffer with the addition of protein. Inhibitor includes buffer, protein, and different concentrations of the inhibitor (the picture shows the highest concentration that was used during the measurement). The reaction rate is defined as the first derivative of the absorption curve with respect to time. The initial reaction rate (max. 10%) is employed in the calculation of Ki'. All measurements are corrected by subtracting the spontaneous CO_2 hydration rate. The measure of CA II with CMP.1 is illustrated as an example.

2.8 Crystallization

2.8.1 Hanging drop method

The method of water vapor diffusion utilising the hanging drop technique was employed for the crystallization of the protein in a complex with inhibitors. The crystallization process was observed using an Olympus SZX10 optical microscope with an Olympus E-620 camera and the QuickPHOTO CAMERA 2.3 software.

The process of crystallization was conducted in two stages. At the begining a solution of CA II protein with a concentration of 25 mg/ml in a buffer with a composition of 50 mM Tris-base - H2SO4, pH 7.8 was mixed with a crystallization buffer (1M Tris-H2SO4, pH 7.8, 1.6M Na citrate) in three different conditions. The ratios were 2:2, 2:1, and 1:2. A similar approach was employed for the CA IX mimic protein, which was dissolved in a 100 mM NaCl and 20 mM Tris-HCl, pH 7.5 buffer. The drops, with a total volume of 3-4 µl, were prepared manually in an EasyXtal® 15-Well Tools plate with X-Seal crystallization supports. The volume of the reservoir solution in the tank was 1,000 microlitres. Crystal formation was finished in 3-6 days. In the subsequent phase, on to crystallization support was applied with 0.2 µl of the inhibitor, which had been dissolved in 100% DMSO, in two separate drops. Subsequently, the drops were subjected to a drying process at 40°C for a duration of 20-40 minutes. Once the initial drop had reduced to 20 nl, 1 µl of crystallization buffer was applied, covering only a small portion of the dried drop. Subsequently, one to three crystals of the protein were transport to the newly formed liquid drop. This was conducted in order to facilitate the dissolution of the inhibitor, which was then able to penetrate the crystals. The final concentration of DMSO in crystallization drops did not exceed **5** % (v/v). The entire crystallization and soaking process was conducted at a temperature of 18° C.

2.9 X-ray data collection method

Prior to data collection, the crystals were soaked for 10 seconds in the reservoir solution, which was supplemented with 20% (v/v) sucrose, and then stored in liquid nitrogen. Measurements for both the CA II and CA IX-mimic complexes with compounds were conducted at an in-house X-ray diffractometer (Rigaku, Japan) at 100 K. The pertinent crystal parameters and data collection statistics are presented in tabular form in the following section

2.10 Structure determination

The crystal structure of both the CA II and CA IX-mimic complexes with compounds were determined by the difference Fourier technique. CA II and CA IX-mimic coordinates from PDB entries 6YZQ [73] and 6T7U [39] were used as models, respectively.

Atomic coordinates of inhibitor molecules were generated by AceDRG program [82]. The information was then written to an mmCIF file, which can be used by the refinement program REFMAC5 [70, 110, 104]. Then, Coot program was used for inhibitor realspace fitting, model rebuilding, and water molecule additions [42]. Refinement was performed using Refmac5 from Ccp4 suite [105], reversing 5% of reflections for cross-validation.

The isotopic atomic displacement parameters (ADPs) were applied for refinement of structures. The quality of the crystallographic model was evaluated by MolProbity [26]. The final refinement statistics are summarised in Table 3.2. All three-dimension structures were generated using PyMol.

2.11 Structural analysis

2.11.1 PyMOL

The visualisation and analysis of the structures of protein-ligand complexes in this study were conducted using the PyMOL Molecular Graphics System, Version 3.0, Schrödinger, LLC software. The primary actions undertaken were as follows:

- Removing water molecules using the right panel: all → hide → waters
- Removing valences using the main menu: display → show valences
- Changing the background color using the main menu: display → background → white
- Select specific region (inhibitor) by clicking on it

- Rename the selected region using the right panel: all→ rename
- Coloring selected region according to the visualization aims using the right panel: selected region → colour → by chain
- For displaing the electronic density maps, the corresponding map files were downloaded and visualised by built-in procedure for map visualization. Used command line: isomesh name, map, 1.0 [level], (selection), 1.5 [buffer], -1 [state], 1.5 [carve]

where name is the name for the new mesh isosurface object; map means the name of the map object to use for computing the mesh; level is the contour level, selection an atom selection about which to display the mesh with an additional "buffer" (if provided); state means the state into which the object should be loaded (default=1) (set state=0 to append new mesh as a new state), and carve is a radius about each atom in the selection for which to include density. If "carve" is not provided, then the whole brick is displayed.

3. RESULTS

3.1 Investigation of inhibitory activity

By the stopped-flow method, it was determined that the inhibitors have binding with high affinity. The values of the inhibition constants of the inhibitors are presented in Table 3.1.

Table 3.1. Results of the inhibitory activity test. The selectivity index was calculated as R= (K_i CA IX)/(K_i CA II), which shows the selectivity of the inhibitor.

Name	**Ki CA II (nM)**	**Ki CA IX (nM)**	**Selectivity index R**
CMP. 1	4.3 ± 1.45	5.2 ± 1.2	0.8
CMP. 2	3.73 ± 0.47	8.9 ± 1.9	0.4
CMP. 3	723.2 ± 64.28	196.1 ± 30.25	3.7

As anticipated, the first two compounds, which are sulfonamides, exhibit low nanomolar inhibition constant values. However, the selectivity index also demonstrates low values. Furthermore, the lower Ki values in the second column of the table indicate that the inhibitor displays enhanced performance for CA II, which is not aligned with the objective of developing CA IX protein-specific inhibitors.

Thiazolidinedione (CMP.3) has been found to exhibit a lower protein binding affinity than sulfonamide inhibitors. This was predicted based on the inhibitor's structural characteristics, which influence its capacity to form bonds with protein amino acid residues, as detailed in Paragraph 5.4 [28]. Nevertheless, the selectivity index for the third compound is the highest among all three inhibitors, which is associated with the much lower values of inhibition for CA IX protein.

Figure 3.1-3.2 illustrates the fit apparent Ki curves obtained in the Williams-Morris plot representation 2.4.

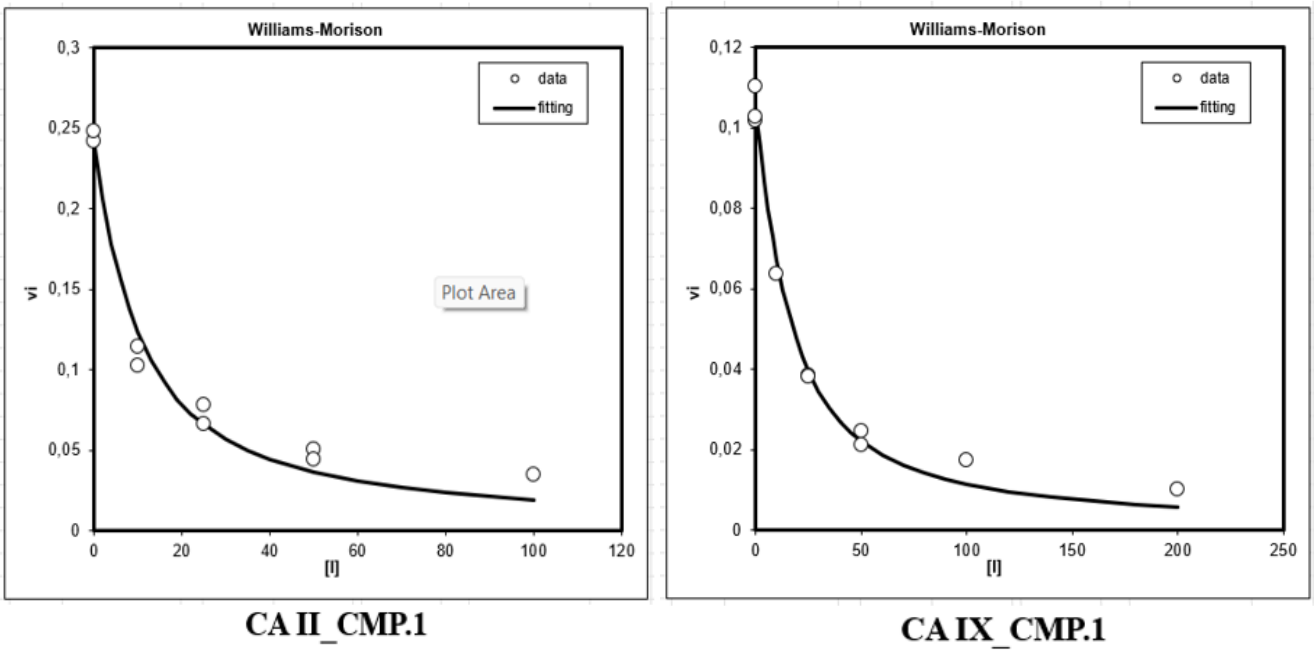

CA II_CMP.1 **CA IX_CMP.1**

Figure 3.1. The data represented on the graphs are the values of several measurements of a single inhibitor concentration. The inhibitor concentrations were within the range from 0.01 mM to 10 mM. The graphs present the concentration of inhibitor (nM) on the abscissa [I] axis and the initial reaction velocity (mol*s^{-1}) on the ordinate [V_i] axis. The value represented by point 0 on the abscissa [I] axis is the velocity of the buffer in the absence of an inhibitor and enzyme. Each measurement was conducted in two to three repetitions.

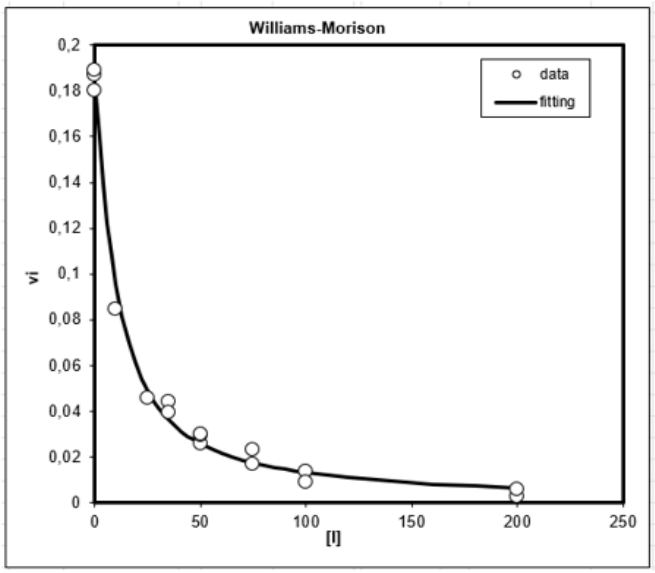

CA II_CMP.2

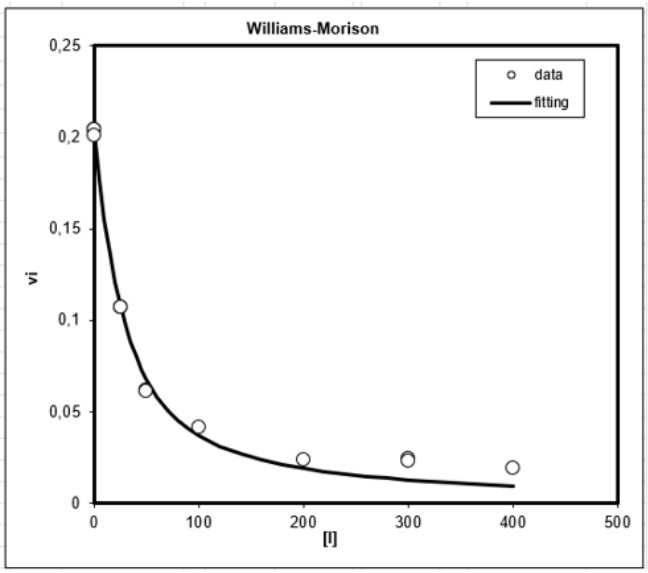

CA IX_CMP.2

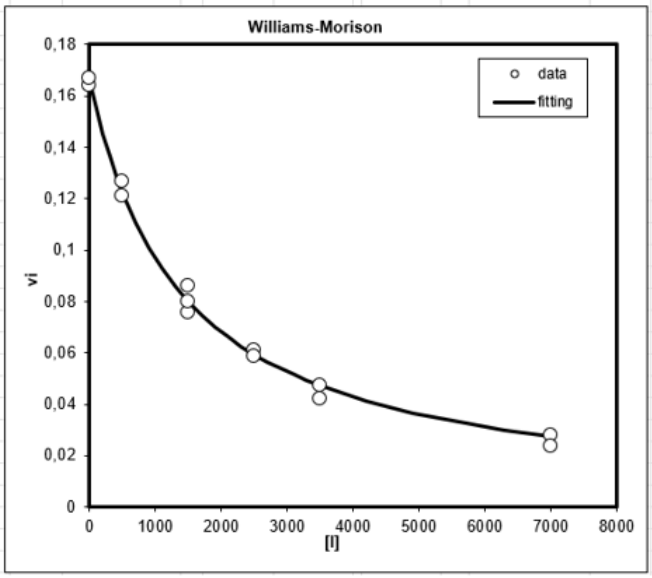

CA II_CMP.3

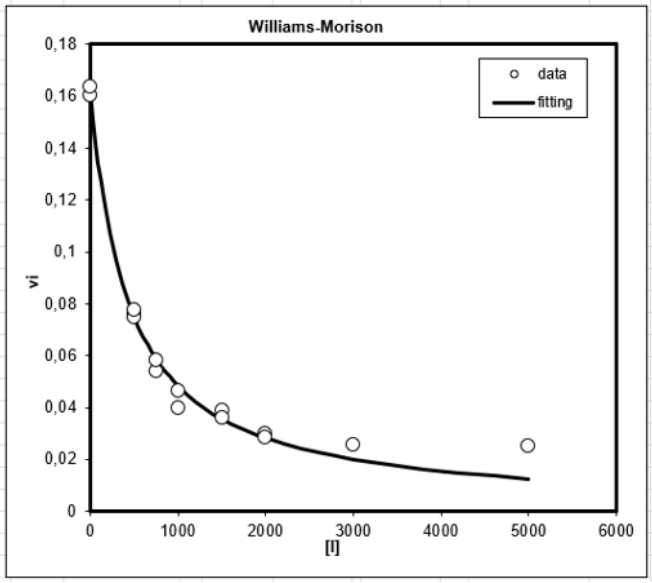

CA IX_CMP.3

Figure 3.2. The data represented on the graphs are the values of several measurements of a single inhibitor concentration. The inhibitor concentrations were within the range from 0.01 mM to 10 mM. The graphs present the concentration of inhibitor (nM) on the abscissa [I] axis and the initial reaction velocity (mol*s^{-1}) on the ordinate [V_i] axis. The value represented by point 0 on the abscissa [I] axis is the velocity of the buffer in the absence of an inhibitor and enzyme. Each measurement was conducted in two to three repetitions.

3.2 Protein - inhibitor complex crystallization

The method described in Section 2.8.1 was successfully employed to crystallize all crystal complexes of the proteins with inhibitors. Following the successful crystallization of these complexes, a UV microscope was used to analyze all positive crystallization events. This analysis was conducted to identify protein crystals by the fluorescence of tryptophan upon excitation with 280 nm UV light. [35].

Figure 3.3 represents photographs of the crystals obtained using optical microscopes (Olympus SZX10, Japan) and a photo camera (Olympus E-620, Japan).

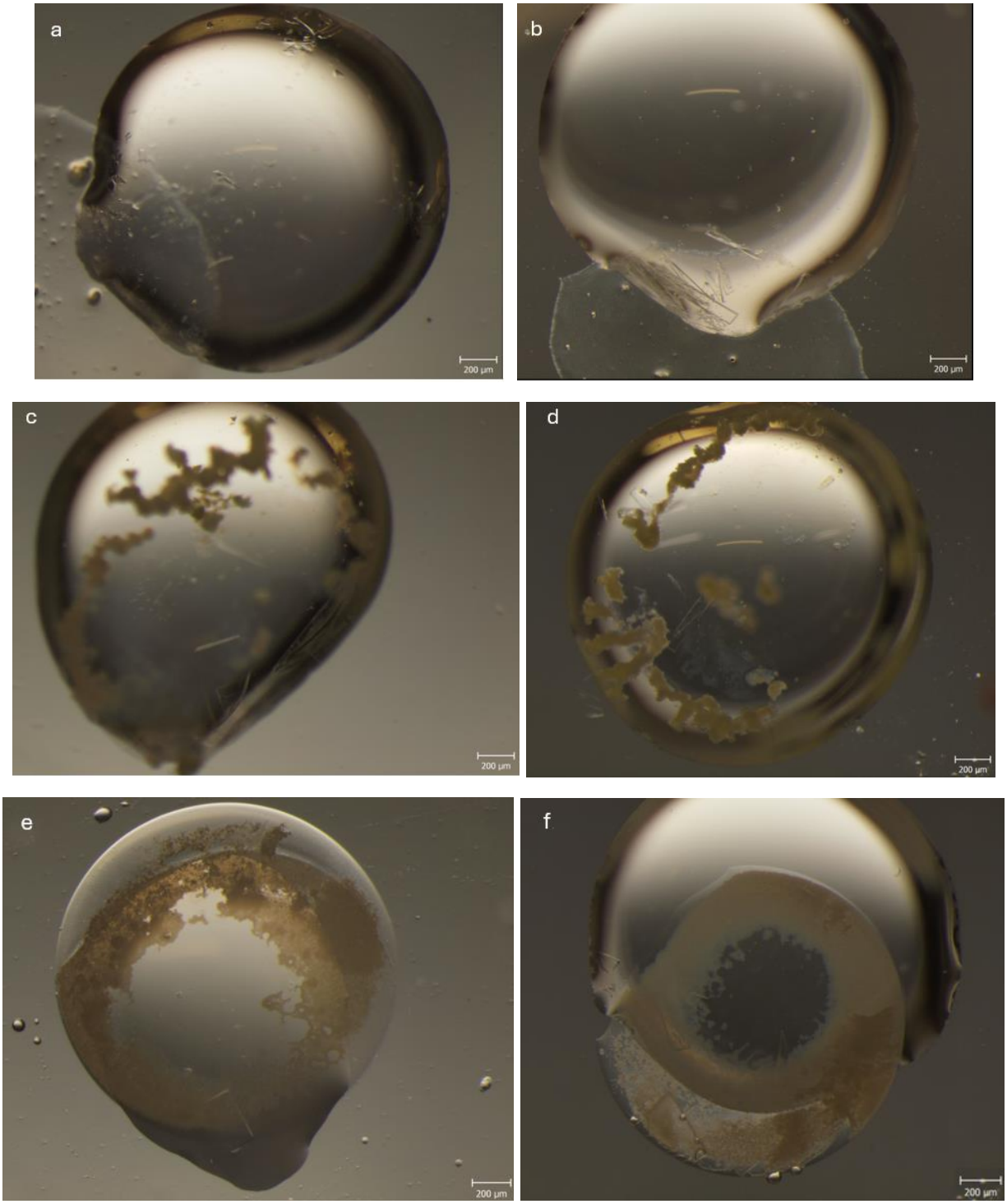

Figure 3.3. Crystals of complexes: a) CAII with CMP.1, b) CA IX(mimic) with CMP.1, c) CAII with CMP.2, d) CA IX (mimic) with CMP.2, e) CA II with CMP.3, f) CA IX(mimic) with CMP.3. The visible spots are the first spot that consisted of the inhibitor dissolved in DMSO and then dried. The length line shown in the pictures.

Then, the ability to bind of the three inhibitors to the active site of carbonic anhydrases was substantiated through enzymatic assays, which demonstrated effective inhibition of the enzyme by all three compounds. The crystals were soaked in a reservoir solution containing 20% (v/v) sucrose and stored in liquid nitrogen for the purpose of data collection. Subsequent X-ray structural analysis of complexes CMP.1, CMP.2, and CMP.3 with CA II and CA IX mimic was conducted to reveal structural information essential for understanding the binding and interaction mechanisms.

3.3 Structure analysis

All crystal of complexes were used to obtain six complete sets of diffraction data using the X-ray diffraction Station at the Institute of Organic Chemistry and Biochemistry, CAS. Crystal parameters and data collection statistics are summarized in Table 3.2, upper part. All structures were determined and refined to resolution below 2 Å, with the best resolution of 1.41 Å for CAIX (mimic) and CMP.2. The statistic from refinement are summarized in Table 3.2, lower part.

To accommodate the inhibitor, the model was rebuilt and water molecules were introduced using a specialized Coot software program. After solvent atoms were added, inhibitor molecules were built in the active site, and several alternate conformations for a number of residues were explored. Compound CMP.1with CAII, and CMP.2 with both proteins were modeled into two alternative conformations with partial occupancies of 0.5 for each conformation in each complex.

Table 3.2. Diffraction data collection and refinement statistics.

CA II in complex with			
	CMP.1	**CMP.2**	**CMP.3**
Data collection statistics			
Wavelength (Å)	1.54	1.54	1.54
Space group	*P2₁*	*P2₁*	*P2₁*
Cell parameters (Å, °)	42.2 41.2 72.1 90.0 104.4 90.0	42.3 41.1 72.1 90.0 104.4 90.0	42.1 41.1 72.1 90.0 104.3 90.0
Resolution range (Å)	50.0-1.50 (1.53- 1.50)	50.0-1.45 (1.49-1.45)	50.0-1.50 (1.54-1.50)
Number of unique reflection	38536 (1856)	42724 (3122)	38373 (2804)
Multiplicity	4.0 (2.4)	6.0 (3.4)	3.2 (1.5)
Completeness (%)	99.6 (97.9)	99.8 (99.3)	99.5 (98.4)
R_{merge} [a]	6.3 (28.4)	4.1 (21.3)	6.6 (45.2)
$CC_{(1/2)}$ (%)	99.8 (85.5)	100 (94.9)	99.8 (71.1)
Average I/σ(I)	11.8 (2.9)	24.4 (4.9)	13.9 (1.8)
Wilson B ($Å^2$)	12.5	18.5	17.9
Refinement statistics			
Resolution range (Å)	25.27- 1.50 (1.53- 1.50)	35.51-1.45 (1.49-1.45)	34.93-1.50 (1.54-1.50)
№. of reflection in working set	36628 (2654)	37458 (1489)	36453 (2660)
№. of reflection in the test set	1887 (134)	1972 (78)	1919 (140)
R_{work} value (%)[b]	15.0 (19.5)	16.5 (24.6)	19.3 (27.2)
R_{free} value (%)[c]	17.5 (20.0)	18.4 (23.1)	20.5 (28.9)
RMSD bond length (Å)	0.010	0.013	0.003
RMSD angle (°)	1.9	1.9	1.2
Mean ADP value ($Å^2$)	12.5	16.9	14.4
Ramachandran plot statistics			
Residues in favored regions (%)	96.1	96.1	96.9
Residues in allowed regions (%)	3.9	3.9	3.1

The data in parentheses refer to the highest-resolution shell.

CA IX in complex with			
	CMP.1	**CMP.2**	**CMP.3**
Data collection statistics			
Wavelength (Å)	1.54	1.54	0.98
Space group	*P2₁*	*P2₁*	*P2₁*
Cell parameters (Å, °)	41.8 41.1 71.8 90.0 103.8 90.0	41.7 41.1 71.8 90.0 103.8 90.0	41.9 41.2 71.9 90.0 103.9 90.0
Resolution range (Å)	50.0 -1.70 (1.73-1.70)	50.0-1.41 (1.44-1.41)	50.0 -1.50 (1.54-1.50)
Number of unique reflection	26136 (1371)	39789 (535)	35483 (2151)
Multiplicity	3.7 (2.1)	2.8 (1.1)	13.2 (11.5)
Completeness (%)	99.5 (98.3)	86.1 (15.9)	92.4 (76.2)
R_{merge} [a]	8.8 (2.8)	2.8 (34.0)	6.5 (48.6)
$CC_{(1/2)}$ (%)	99.3 (85.3)	99.9 (76.1)	99.8 (68.4)
Average I/σ(I)	9.1 (2.9)	21.2 (1.7)	12.9 (1.9)
Wilson B ($Å^2$)	19.2	19.3	19.1
Refinement statistics			
Resolution range (Å)	25.21 -1.70 (1.73-1.70)	40.55-1.41 (1.44-1.41)	31.99-1.50 (1.54-1.50)
№. of reflection in working set	24819 (1801)	28781 (224)	33708 (2034)
№. of reflection in the test set	1303 (87)	1515 (12)	1775 (108)
R_{work} value (%)[b]	14.8 (18.5)	14.2 (23.2)	18.7 (25.6)
R_{free} value (%)[c]	19.5 (25.4)	17.7 (28.2)	21.6 (26.5)
RMSD bond length (Å)	0.011	0.010	0.008
RMSD angle (°)	1.8	1.75	1.7
Mean ADP value ($Å^2$)	13.9	13.8	17.6
Ramachandran plot statistics			
Residues in favored regions (%)	96.9	97.3	97.3
Residues in allowed regions (%)	3.2	2.8	2.8

Multiplicity means number of total reflections / number of unique reflections.

R_{merge} [a] = ($|I_{hkl} - \langle I \rangle|$)/Ihkl, where the average intensity <I> is taken over all symmetry equivalent measurements and Ihkl is the measured intensity for any given reflection.

R_{value} [b] = $||F_o| - |F_c||/|F_o|$, where F_o and F_c are the observed and calculated structure factors, respectively.

Rfree is equivalent to the R-value but is calculated for 5% of the reflections chosen at random and omitted from the refinement process.

The quality of the crystallographic model was evaluated using the MolProbity software.

All crystals belong to monoclinic $P2_1$ space group. The highest quality refinement statistics (R_{free} and R_{work}) were achieved for the high-resolution structure of CAIX (mimic) with CMP.2.

3.4 Description of inhibitor binding

To investigate the interaction of inhibitors with the active site of enzymes, determined crystal structure of CAII and CAIX-mimic by X-ray crystallography. The results were visualized using PyMOL (Molecular Graphics System, Version 3.0 Schrödinger, LLC).

Figure 3.4, illustrates detail wiew into the active site of CA II and CA IX with bound inhibitors, as derived from the coordinates of the obtained crystal structures.

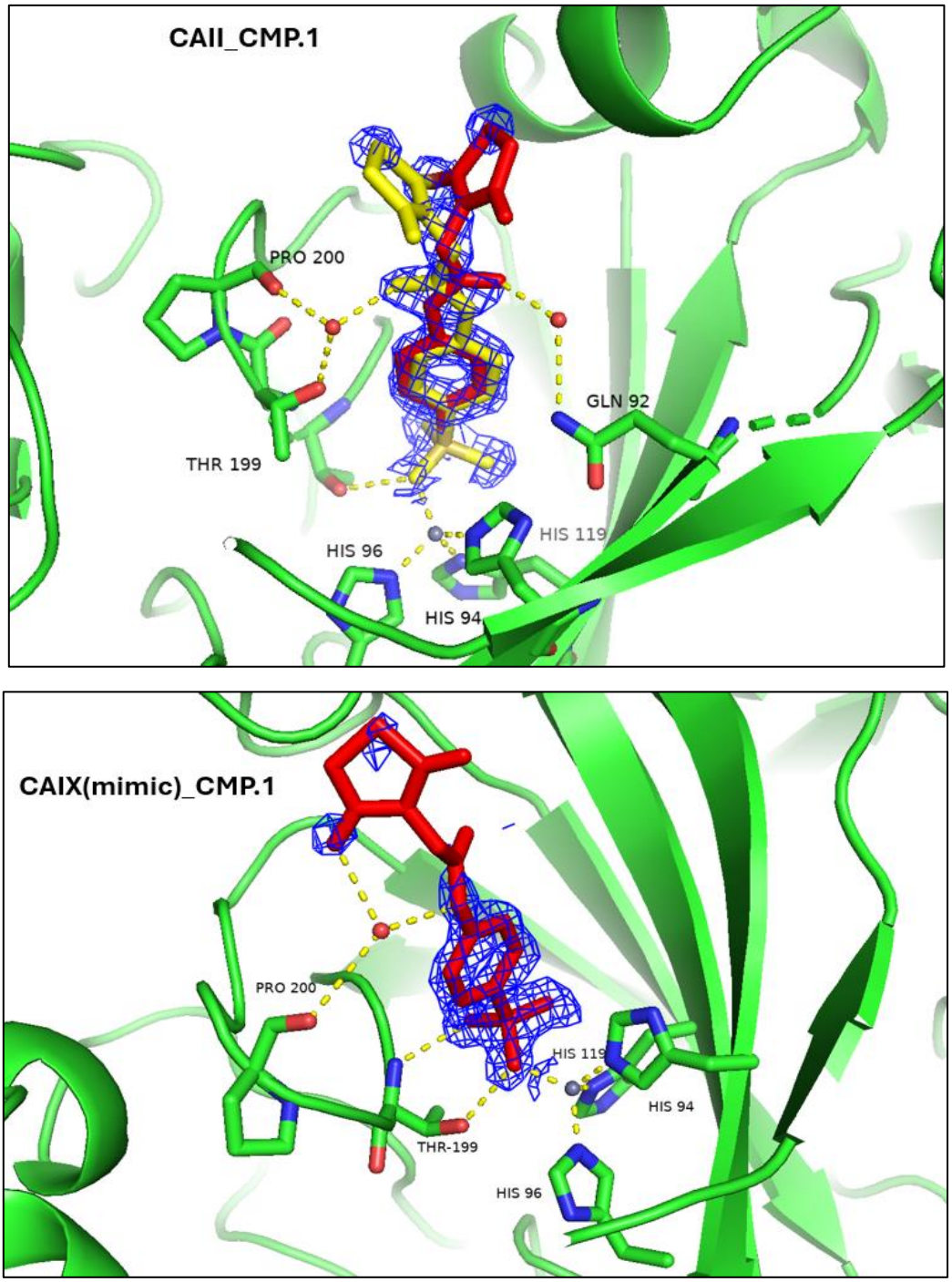

Figure 3.4. A) CMP.1. The Crystal structures of proteins in complex with inhibitors. The zinc ion is indicated by a gray sphere coordinated by three histidine residues. Carbon atoms are highlighted in green, nitrogen in blue, and oxygen in red. Water molecules are shown as red spheres. Hydrogen bonds are represented by yellow dashed lines. The figure was created using the PyMOL software.

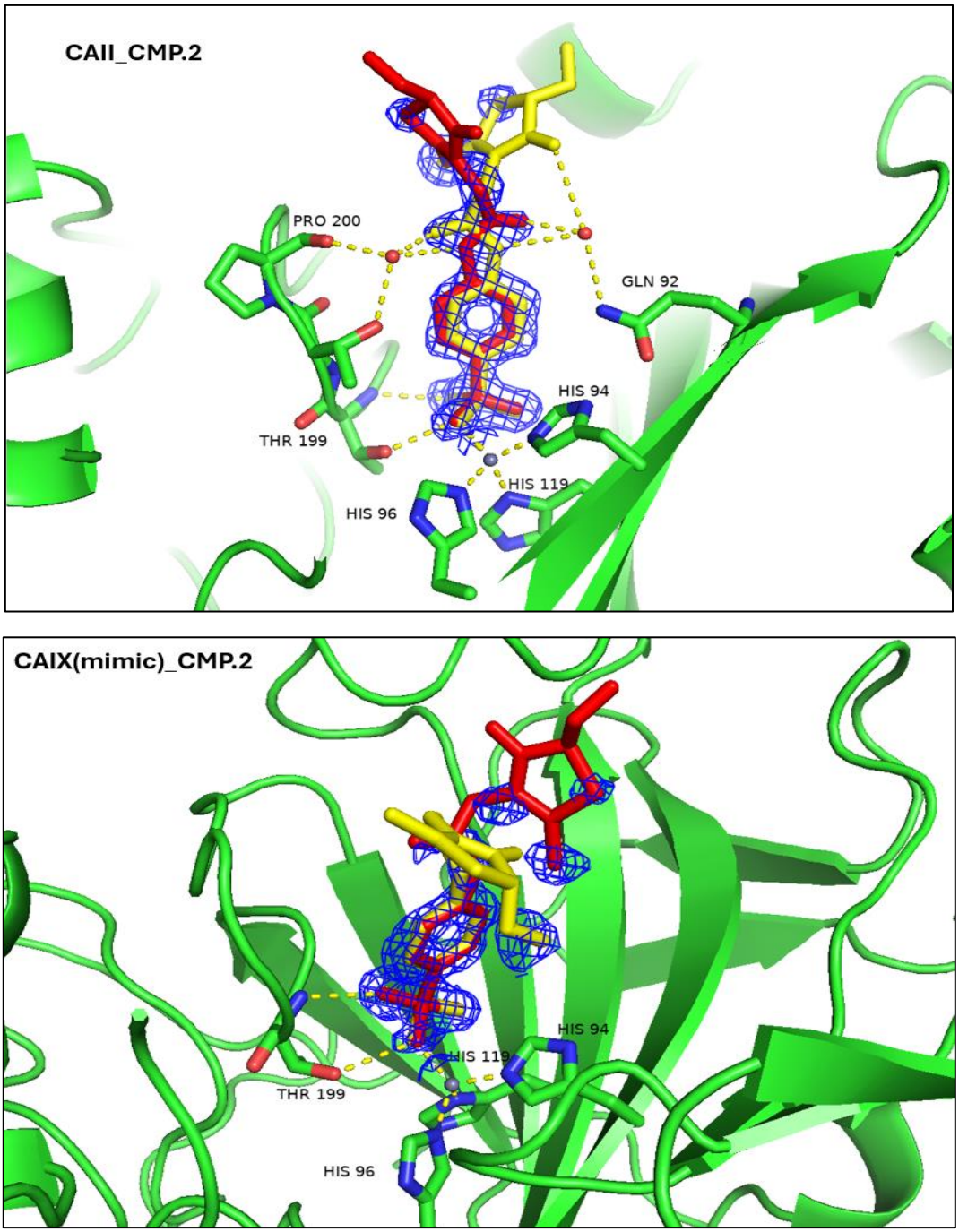

Figure 3.4. B) CMP.2. The Crystal structures of proteins in complex with inhibitors. The zinc ion is indicated by a gray sphere coordinated by three histidine residues. Carbon atoms are highlighted in green, nitrogen in blue, and oxygen in red. Water molecules are shown as red spheres. Hydrogen bonds are represented by yellow dashed lines. The figure was created using the PyMOL software.

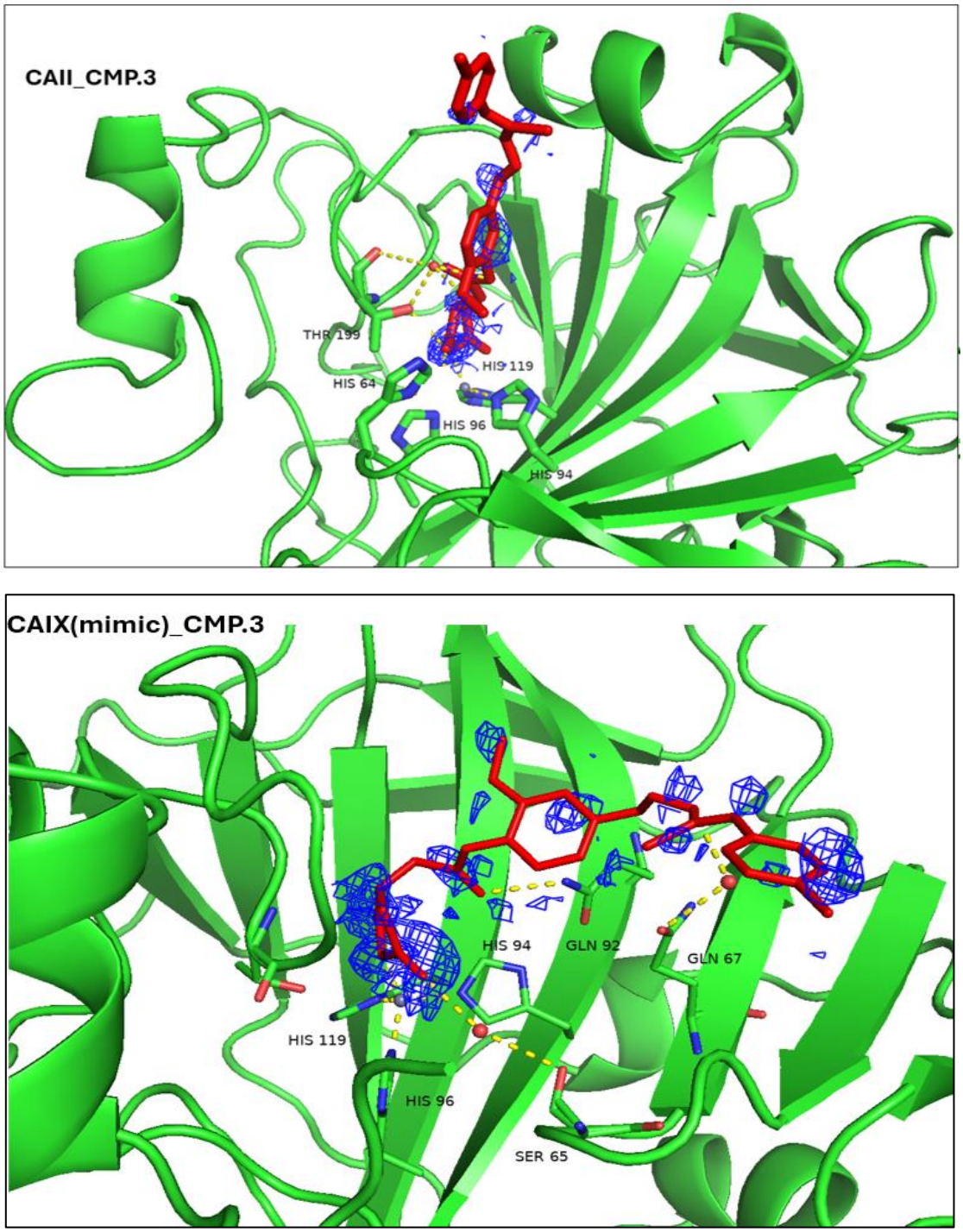

Figure 3.4. C) CMP.3. The Crystal structures of proteins in complex with inhibitors. The zinc ion is indicated by a gray sphere coordinated by three histidine residues. Carbon atoms are highlighted in green, nitrogen in blue, and oxygen in red. Water molecules are shown as red spheres. Hydrogen bonds are represented by yellow dashed lines. The figure was created using the PyMOL software.

All the shown polar bonds here do not exceed 3 Å. The figures show zinc coordination by three histidine residues His94, His96, His119 for CA II for CA IX (mimic). The fourth interaction in the coordinated sphere of the ion, which is intended for binding the substrate of the ion in the case of inhibition, is occupied by an inhibitor nitrogen atom. The binding of the inhibitor to $zinc^{2+}$ is facilitated by an deprotonated amide group with free electron pair, a common feature among all inhibitors. In compounds CMP.1 and CMP.2, which are sulfonamides, an additional hydrogen ion of the amide group is present. As illustrated in Figure 3.3, this ion engages in a polar interaction with the side chain of the amino acid residue Thr 199. Additionally, the amino group of the threonine 199 main chain forms a hydrogen bond with the oxygen from the sulfonamide residue. CMP.3 which is thiazolidinedione does not form a connection with the oxygen of Thr 199 and does not perform a polar interaction with a residue in the absence of a second hydrogen ion. However, the amide group allows for a connection to be formed with the $zinc^{2+}$ ion.

CAII_CMP.1 As shown in Figure 3.4, the inhibitor in this complex can occupy two positions due to bond formation, where a water molecule bridges the space between the inhibitor amino acid residues. The linker fragment, situated after the six-membered aromatic ring (also known as the "body"), interacts with water molecules in both positions. In one instance of the inhibitor's positioning, the linker is connected to Thr199 and Pro200 via water. The second variant of the inhibitor's location in the active site of carbonic anhydrase II is stabilized by a bond between the linker fragment, water, and Gln92.

CAIX(mimic)_CMP.1 Following the analysis of the X-ray crystallography results, it became evident that in addition to the primary bonds of the compound's head, two additional bonds are formed between different parts of the compound and a water molecule. The water molecule is then bonded to the amino acid residue Pro200.

CAII_CMP.2. The inhibitor molecule is presented as a complete molecule, and the compound can exist in two different conformations. Considering the first conformation, it is evident that the inhibitor is stabilized within the linker fragment of the compound, with

residues Pro200 and Thr199, through a water molecule. In the second variant, the tail and linker are connected to a water molecule, which in turn forms a bond with Gln92.

CAIX(mimic)_CMP.2. This complex is identical to the CAII_CMP.2 complex. The molecule is depicted in its entirety and, as illustrated in Figure 3.3, can exist in two distinct conformations. However, it is only bonded to the zinc^{2+} ion, the polar interaction, and the hydrogen bond with the amino acid residue Thr199.

CAII_CMP.3 In addition to the primary nitrogen-zinc bond, the complex of thiazolidinedione and CA II protein also exhibits a stabilizing bond between the compound and a water molecule bound to Thr199.

CAIX(mimic)_CMP.3. In the complex of carbonic anhydrase IX protein and inhibitor CMP.3, along with the main bond, one water bond with Ser65 and another water bond with Gln67 are also observed. Furthermore, a direct bond of the compound with amino acid residue Gln92 is evident.

3.5 Discussion

The objective of this study was to investigate the specific binding of selected inhibitors to carbonic anhydrase IX. ISpecific inhibition of CA IX represents a significant area of interest, given the role of this protein in oncogenesis. Additionally, carbonic anhydrase II is included in this study as the most abundant "off-target" indicator due to its extensive distribution throughout the human body. Two of the selected inhibitors were sulfonamides, while the third was a thiazolidinedione.

First, *in vitro* measurements were performed, during which the inhibitory effect of the compounds on the enzymatic activity of the CA IX and CA II proteins was observed, using the stopped-flow method (section 2.7.1). As shown in Table 3.1, the inhibition constants for sulfonamides ranged from 3.73 ± 0.74 nM to 8.9 ± 1.9 nM, while the thiazolidinedione inhibitor had values of 723.2 ± 64.28 nM for CAII and 196.1 ± 30.25 nM for

CAIX. The most effective inhibition result was observed for CMP.2 and CA II 3.73 ± 0.47 nM. It is known that these values are predicted because sulfonamides are the most effective class of inhibitory compounds for carbonic anhydrases, with the best inhibitory effect [93].

It should be noted that the inhibitory capacity of triazolidinedione is lower than that of sulfonamides. This is due to the presence of only one hydrogen atom that forms a bond with the Zn^{2+} ion and the absence of a second hydrogen ion, which is present in sulfonamides. The absence of a second hydrogen ion as in sulfonamides, which formas an additional bond a polar interaction with the side chain of the amino acid residue Thr 199 also plays the role. Furthermore, the absence of a hydrogen bond from oxygen to the main chain of threonine 199 is likely due to lower binding affinity of this type of compound. The ring be located 3.7 Å from the nitrogen atom of the Thr199 backbone, which makes it challenging to form a bond [28]. However, CMP.3 demonstrates the highest degree of selectivity. It is nearly four times more effective at inhibiting the target protein of this project, CAIX over CAII.

To gain further insight into the binding of selected inhibitors to carbonic anhydrase, X-ray analysis was conducted next. Given the difficulty in crystallizing the CAIX protein, a CAIX mimic protein prepared in the Structural Biology Laboratory at the Institute of Organic Chemistry and Biochemistry, CAS, was utilized for this portion of the work. Modifications were made to the protein in order to facilitate crystallization crystallization while retain the active site of CAIX. The prepared crystals (section 2.8.1) were measured using the X-ray data collection method, which provided valuable insight into the interactions on atomic level of the inhibitors in the active site pocket of CAII and CAIX. All structures were determined and refined to a resolution below 2 Å, with the best resolution of 1.41 Å for CAIX mimic in complex with CMP.2. Further structural analysis (Table 3.2) of the obtained data revealed important interactions between the inhibitors and the amino

acid residues of the active site of the proteins. The images of the inhibitor-protein complexes, created in PyMOL, provide a visual representation of these interactions (section 3.5).

From this visualization, it was revealed that CMP.1 which is sulfonamide, has the potential to existbinds the active site in two alternative conformations, each of which is stabilized by two bonds to the amino acids of the protein through water molecules. In contrast, the CAIX(mimic)_CMP.1 complex revealed that the compound can not exist in twoaquires single conformations but and can forms a bond with Pro200, thereby stabilizing the compound.

The second sulfonamide, CMP.2, is present in two conformations in both protein complexes. CMP.2 is stabilized by two bonds to three residues (Gln92, Thr199, Pro200) through water, in addition to the main bonds from the inhibitor head, when it is present with CAII. However, in CAIX, the inhibitor is exclusively bound to the protein by the main bonds from the sulfonamide head. The second hydrogen ion engages in a polar interaction with the side chain of the amino acid residue Thr 199, the amino group of the threonine 199 main chain forms a hydrogen bond with the oxygen from the sulfonamide residue, and nitrogen bound Zn^{2+} ion.

CMP.3 binds in a sigle conformation into the CAII, in addition to the primary nitrogen bond of the compound with the zinc^{2+} ion present in the active site of the protein. This bond with the amino acid residue Thr199 is facilitated by the involvement of water. However, this inhibitor with CAIX has three polar interactions with Gln92, Gln67, Ser 65: two of which are carried out through water, and one is direct. This ensures the optimal stabilization of the inhibitor, which in turn ensures its optimal inhibitory effect on the protein.

The selectivity of inhibitors for CAII and CAIX is influenced by the amino acid residue Phe130 present in the CAII protein structure and replaced by Val in CAIX. In the

case of sulfonamide inhibitors, the residue does not present a problem for the compounds. However, this is a crucial factor for thiazolidinediones. The protruding residue in the CAII molecule establishes a specific position for the inhibitor, which is supported by a single bond. The absence of this residue in the CAIX protein structure allows the inhibitor to occupy a more conformationally favorable position, forming three stabilizing bonds.

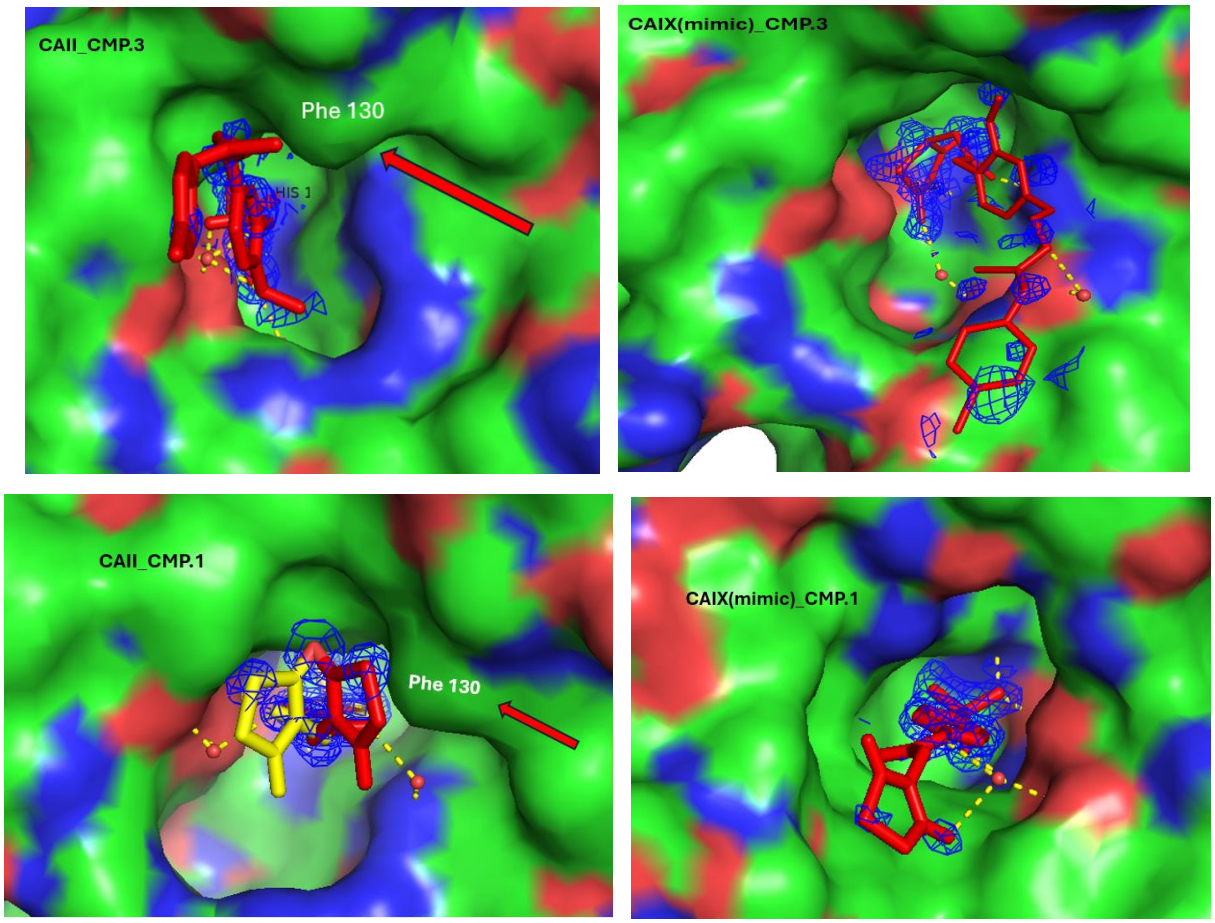

Figure 3.5. A) Illustration of the critical role of residue Phe130 for thiazolidinedione and sulfonamide inhibitor (CMP.1).

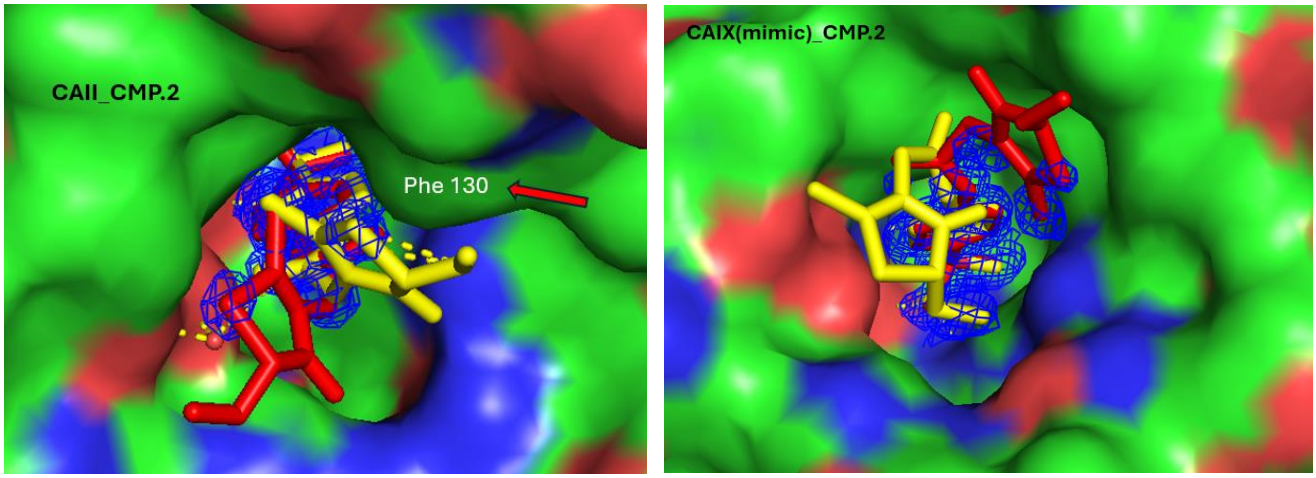

Figure 3.5. B) Illustration of the critical role of residue Phe130 for sulfonamide inhibitor (CMP.2).

It can be concluded that CMP.3 is the most selective inhibitor for CAIX among the compounds explored in this work. Its selectivity index is the highest among those measured, which ensures targeted inhibition while minimizing the likelihood of binding to other metalloenzymes. The presence of the largest number of bonds with the protein has the greatest impact on protein function.

It is therefore important to continue developing and potentially modifying these inhibitors.

CONCLUSION

A summary of information on human carbonic anhydrases was prepared based on a review of relevant literature in this thesis. The physiological functions and further participation of individual CA isoenzymes in pathological processes also were presented in detail. The structure of the active site of metalloenzymes and their catalytic mechanism were reviewed. Particular focus was put on carbonic anhydrases II and IX. CA IX isoenzyme has been identified as a potential tumor marker and target for tumor diagnosis and treatment. CA II was considered an "off-target" protein. Additionally, a summary of potential methods for inhibiting carbonic anhydrases was provided.

After the experimental part of this thesis can be concluded:

1. The inhibitory properties of three selected inhibitors towards CA II and CAIX were evaluated by stopped-flow method and X-ray crystallography method for which the crystalls were previously grown. These inhibitors belong to the sulfonamides and thiazolidinediones.

2. It was demonstrated that the inhibitory capacity of triazolidinedione is inferior to that of sulfonamides.

3. Kinetic studies have shown that the inhibitors have a high affinity for protein and are very effective in reducing enzymatic activity. The most effective inhibition result was observed for CMP.2 and CA II 3.73 ± 0.47 nM.

4. The X-ray structural study, aimed at complexes of three inhibitors with two proteins, revealed the structular basis explaining high affinity and specificity of binding for each of studied compounds. All structures were determined and refined to a resolution below 2 Å, with the best resolution of 1.41 Å for CAIX mimic in complex with CMP.2

5. It has been demonstrated that certain inhibitors are capable of occupying the active site of proteins in two distinct conformations.

6. It was further revealed that the ability to bind to the active site of the two different proteins was influenced by the amino acid residue Phe 130, thereby ensuring the selectivity of these CA IX-targeted inhibitors.

These results are relevant for further studies of these compounds.

REFERENCES

1. Aggarwal M, Boone CD, Kondeti B, McKenna R (2013) Structural annotation of human carbonic anhydrases. *Journal of Enzyme Inhibition and Medicinal Chemistry* 28(2): 267–277. DOI: 10.3109/14756366.2012.737323, PMID: 23137351.

2. Akisawa Y, Nishimori I, Taniuchi K, *et al* (2003) Expression of carbonic anhydrase-related protein CA-RP VIII in non-small cell lung cancer. *Virchows Arch* 442 (1): 66–70. DOI: 10.1007/s00428-002-0721-y , PMID: 12536316.

3. Almstahl A, Wikstrom M (2003) Electrolytes in stimulated whole saliva in individuals with hyposalivation of different origins. *Arch Oral Biol* 48 (5): 337–344. DOI: 10.1016/s0003-9969(02)00200-5 .

4. Alterio V, Di Fiore A, D'Ambrosio K, *et al* (2012) Multiple binding modes of inhibitors to carbonic anhydrases: how to design specific drugs targeting 15 different isoforms? *Chem Rev* 112 (8): 4421–4468. DOI: 10.1021/cr200176r , PMID: 22607219.

5. Alterio V, Hilvo M, Fiore AD, Supuran T, Pan P, *et al* (2009) Crystal structure of the catalytic domain of the tumor-associated human carbonic anhydrase IX. *Proc Natl Acad Sci U S A* 106 (38): 16233-16238. DOI: 10.1073/pnas.0908301106 , PMCID: PMC2752527 , PMID: 19805286.

6. Ames S, Pastorekova S, Becker HM (2018) The proteoglycan-like domain of carbonic anhydrase IX mediates non-catalytic facilitation of lactate transport in cancer cells. *Oncotarget* 9 (46): 27940–27957. DOI: 10.18632/oncotarget.25371.

7. Aspatwar A, Tolvanen ME, Parkkila S (2013) An update on carbonic anhydrase-related proteins VIII, X and XI. *J Enzyme Inhib Med Chem* 28 (6): 1129–1142. DOI: 10.3109/14756366.2012.727813 , PMID: 23294106.

8. Aspatwar A, Tolvanen MEE, Barker H, Syrjänen L, Valanne S, Purmonen S, Waheed A, Sly WS, Parkkila S (2022) Carbonic anhydrases in metazoan model organisms: molecules, mechanisms, and physiology. *Physiol Rev* 102 (3): 1327–1383. DOI: 10.1152/physrev.00018.2021 , PMID: 35166161.

9. Avvaru BS, Kim CU, Sippel KH, Gruner SM, Agbandje-McKenna M, Silverman DN *et al* (2010) A short, strong hydrogen bond in the active site of human carbonic anhydrase II. *Biochemistry* 49 (2): 249–251. DOI: 10.1021/bi902007b , PMCID: PMC2810610, PMID: 20000378.

10. Baine MJ, Chakraborty S, Smith LM, *et al* (2011) Transcriptional profiling of peripheral blood mononuclear cells in pancreatic cancer patients identifies novel genes with potential diagnostic utility. *PLoS One* 6 (2):e17014. DOI: 10.1371/journal.pone.0017014 , PMCID: PMC3037404, PMID: 21347333.

11. Baine MJ, Menning M, Smith LM, *et al* (2011) Differential gene expression analysis of peripheral blood mononuclear cells reveals novel test for early detection of pancreatic cancer. *Cancer Biomark* 11 (1): 1–14. DOI: 10.3233/CBM-2012-0260 , PMCID: PMC3557848 , PMID: 22820136.

12. Bataller L, Sabater L, Saiz A, *et al* (2004) Carbonic anhydrase-related protein VIII: autoantigen in paraneoplastic cerebellar degeneration. *Ann Neurol* 56 (4): 575–579. DOI: 10.1002/ana.20238 , PMID: 15389893.

13. Bayram E, Senturk M, Kufrevioglu OI, Supuran CT (2008) In vitro inhibition of salicylic acid derivatives on human cytosolic carbonic anhydrase isozymes I and II. *Bioorg Med Chem* 16 (20): 9101–9105. DOI: 10.1016/j.bmc.2008.09.028 , PMID: 18819808.

14. Beckman KA, Luchs J, Milner MS (2016) Making the diagnosis of Sjogren's syndrome in patients with dry eye. *Clin Ophthalmol* 10: 43–53. DOI: 10.2147/OPTH.S80043 , PMCID: PMC4699514.

15. Bonneau A, Maresca A, Winum JY, Supuran CT (2013) Metronidazole-coumarin conjugates and 3-cyano-7-hydroxy-coumarin act as isoform-selective carbonic anhydrase inhibitors. *J Enzyme Inhib Med Chem* 28 (2): 397–401. DOI: 10.3109/14756366.2011.650692, PMID: 22299576.

16. Boriack-Sjodin PA, Heck RW, Laipis PJ, Silverman DN, Christianson DW (1995) Structure determination of murine mitochondrial carbonic anhydrase V at 2.45-A resolution: implications for catalytic proton transfer and inhibitor design. *Proc Natl Acad Sci USA* 92 (24): 10949–10953. DOI: 10.1073/pnas.92.24.10949.

17. Borras J, Scozzafava A, Menabuoni L, *et al* (1999) Carbonic anhydrase inhibitors. Synthesis of water-soluble, topically effective intraocular pressure lowering aromatic/heterocyclic sulfonamides containing 8-quinoline-sulfonyl moieties: is the tail more important than the ring? *Bioorg Med Chem* 7:2397–2406. DOI: 10.1016/s0968-0896(99)00190-x , PMID: 10632049.

18. Briganti F, Mangani S, Orioli P, Scozzafava A, Vernaglione G, Supuran C T (1997) Carbonic anhydrase activators: X-ray crystallographic and spectroscopic investigations for the interaction of isozymes I and II with histamine . *Biochemistry* 36(34): 10384–10392. DOI: 10.1021/bi970760v .

19. Canto de Souza L, Provensi G, Vullo D, *et al* (2017) Carbonic anhydrase activation enhances object recognition memory in mice through phosphorylation of the extracellular signal-regulated kinase in the cortex and the hippocampus. *Neuropharmacology* 118: 148–156. DOI: 10.1016/j.neuropharm.2017.03.009 , PMID: 28286213.

20. Capasso C, Supuran CT (2015) An overview of the alpha-, beta- and gamma-carbonic anhydrases from Bacteria: can bacterial carbonic anhydrases shed new light on evolution of bacteria? *J Enzyme Inhib Med Chem* 30 (2): 325–332. DOI: 10.3109/14756366.2014.910202 , PMID: 24766661

21. Carta F, Maresca A, Scozzafava A, *et al* (2015) 5- and 6-membered (thio)lactones are prodrug type carbonic anhydrase inhibitors. *Bioorg Med Chem Lett* 22 (1): 267–270. DOI: 10.1016/j.bmcl.2011.11.018 .

22. Carta F, Temperini C, Innocenti A, *et al* (2010) Polyamines inhibit carbonic anhydrases by anchoring to the zinc-coordinated water molecule. *J Med Chem* 53 (15): 5511–5522. DOI: 10.1021/jm1003667 .

23. Carta F, Vullo D, Maresca A, *et al* (2013) Mono-/dihydroxybenzoic acid esters and phenol pyridinium derivatives as inhibitors of the mammalian carbonic anhydrase isoforms I, II, VII, IX, XII and XIV. *Bioorg Med Chem* 21 (6): 1564–1569. DOI: 10.1016/j.bmc.2012.05.019 , PMID: 22668600.

24. Carter WG, Vigneswara V, Newlaczyl A, *et al* (2015) Isoaspartate, carbamoyl phosphate synthase-1, and carbonic anhydrase-III as biomarkers of liver injury. *Biochem Biophys Res Commun*. 458(3):626–631. DOI: 10.1016/j.bbrc.2015.01.158 , PMCID: PMC4355035 , PMID: 25684186.

25. Cerami E, Gao J, Dogrusoz U, *et al* (2012) The cBio cancer genomics portal: an open platform for exploring multidimensional cancer genomics data. *Cancer Discov* 2 (5): 401–404. DOI: 10.1158/2159-8290.CD-12-0095 , PMCID: PMC3956037 , PMID: 22588877.

26. Chen VB, Arendall WB 3rd, Headd JJ, Keedy DA, Immormino RM, Kapral GJ, Murray LW, Richardson JS, Richardson DC (2009) MolProbity: all-atom structure validation for macromolecular crystallography. *Acta Crystallogr D Biol Crystallogr* 66 (1): 12-21. doi: 10.1107/S0907444909042073. Epub 2009 Dec 21. PMID: 20057044; PMCID: PMC2803126.

27. Christianson DW, FierkeCA (1996) Carbonic Anhydrase: Evolution of the Zinc Binding. *Acc Chem Res* 29 (7): 331-339. DOI: 10.1021/ar9501232

28. Chrysanthopoulos PK, Mujumdar P, Woods LA, Dolezal O, Ren B, Peat TS, Poulsen SA (2017) Identification of a New Zinc Binding Chemotype by Fragment Screening. *J Med Chem* 60 (17): 7333-7349. doi: 10.1021/acs.jmedchem.7b00606. Epub 2017 Sep 1. PMID: 28817930.

29. Chu X, Zhao P, Lv Y, *et al* (2016) Expression of carbonic anhydrase-9 correlates with metastasis and prognosis of Chinese patients with invasive breast ductal carcinoma. *Int J Clin Exp Pathol* 9 (2): 1446–1452.

30. Cianchi F, Vinci MC, Supuran CT, Peruzzi B, De Giuli P, Fasolis G, *et al* (2010) Selective inhibition of carbonic anhydrase IX decreases cell proliferation and induces ceramide-mediated apoptosis in human cancer cells. *J Pharmacol Exp Ther* 334 (3): 710–719. DOI: 10.1124/jpet.110.167270, PMID: 20519553.

31. D'Ambrosio K, Carradori S, Monti SM, *et al* (2015) Out of the active site binding pocket for carbonic anhydrase inhibitors. *Chem Commun* 51 (2): 302–305. DOI: 10.1039/C4CC07320G.

32. Davis RA, Hofmann A, Osman A, *et al* (2011) Natural product-based phenols as novel probes for mycobacterial and fungal carbonic anhydrases. *J Med Chem* 54 (6): 1682–1692. DOI: 10.1021/jm1013242 , PMID: 21332115.

33. De Simone G, Alterio V, Supuran CT (2013) Exploiting the hydrophobic and hydrophilic binding sites for designing carbonic anhydrase inhibitors. *Expert Opin Drug Discov* 8 (7): 793–810. DOI: 10.1517/17460441.2013.795145 , PMID: 23627619.

34. Di Fiore A, Monti SM, Hilvo M, Parkkila S, Romano V, Scaloni A, *et al* (2009) Crystal structure of human carbonic anhydrase XIII and its complex with the inhibitor acetazolamide. *Proteins* 74 (1): 164–175. DOI: 10.1002/prot.22144 , PMID: 18618712.

35. Dierks K, Meyer A, Oberthür D, Rapp G, Einspahr H & Betzel C (2010) Efficient UV detection of protein crystals enabled by fluorescence excitation at wavelengths longer than 300 nm. *Acta Crystallograph Sect F Struct Biol Cryst Commun* 66: 478–484. DOI: 10.1107/S1744309110007153 .

36. Dodgson SJ, Forster RE 2nd, Storey BT, *et al* (1980) Mitochondrial carbonic anhydrase. *Proc Natl Acad Sci U S A* 77 (9): 5562–5566. DOI: 10.1073/pnas.77.9.5562 , PMCID: PMC350102 , PMID: 6776540.

37. Domsic JF, Avvaru BS, Kim CU, Gruner SM, *et al* (2008) Entrapment of Carbon Dioxide in the Active Site of Carbonic Anhydrase II. *J Biol Chem* 283 (45): 30766 – 30771. DOI: 10.1074/jbc.M805353200 , PMID: 18768466.

38. Duda DM, Tu C, Fisher SZ, An H, Yoshioka C, Govindasamy L, *et al* (2005) Human carbonic anhydrase III: structural and kinetic study of catalysis and proton transfer. *Biochemistry* 44 (30): 10046–10053. DOI: 10.1021/bi050610h , PMID: 16042381.

39. Dvořanová J, Kugler M, Holub J, Šícha V, Das V, Nekvinda J, El Anwar S, Havránek M, Pospíšilová K, Fábry M, Král V, Medvedíková M, Matějková S, Lišková B, Gurská S, Džubák P, Brynda J, Hajdúch M, Grüner B, Řezáčová P (2020) Sulfonamido carboranes as highly selective inhibitors of cancer-specific carbonic anhydrase IX. *Eur J Med Chem* 15;200:112460. doi: 10.1016/j.ejmech.2020.112460. Epub 2020 May 18. PMID: 32505851.

40. Ekinci D, Karagoz L, Ekinci D, *et al* (2013) Carbonic anhydrase inhibitors: in vitro inhibition of α isoforms (hCA I, hCA II, bCA III, hCA IV) by flavonoids. *J Enzyme Inhib Med Chem* 28 (2): 283–288. DOI: 10.3109/14756366.2011.643303 , PMID: 22168126.

41. Elder I, Fisher Z, Laipis PJ, Tu C, McKenna R, Silverman DN (2007) Structural and kinetic analysis of proton shuttle residues in the active site of human carbonic anhydrase III. *Proteins* 68 (1): 337–343. DOI: 10.1002/prot.21403 , PMID: 17427958.

42. Emsley P, Cowtan K (2004) Coot: model-building tools for molecular graphics. *Acta Crystallogr D Biol Crystallogr* 60 (Pt12 Pt1): 2126-2132. doi: 10.1107/S0907444904019158. Epub 2004 Nov 26. PMID: 15572765.

43. Ferraroni M, Carta F, Scozzafava A, Supuran CT (2015) Thioxocoumarins inhibit carbonic anhydrases through a different mechanism compared to coumarins. *J Med Chem* 59 (1): 462-473. DOI: 10.1021/acs.jmedchem.5b01720 , PMID: 26688270.

44. Gao BB, Clermont A, Rook S, Fonda SJ, Srinivasan VJ, Wojtkowski M, Fujimoto JG, *et al* (2007) Extracellular carbonic anhydrase mediates hemorrhagic retinal and cerebral vascular permeability through prekallikrein activation. *Nat. Med* 13 (2): 181–188. DOI: 10.1038/nm1534 , PMID: 17259996.

45. Gao J, Aksoy BA, Dogrusoz U, *et al* (2013) Integrative analysis of complex cancer genomics and clinical profiles using the cBioPortal. *Sci Signal* 6 (269):pl1. DOI: 10.1126/scisignal.2004088 , PMCID: PMC4160307 .

46. Genega EM, Ghebremichael M, Najarian R, *et al* (2010) Carbonic anhydrase IX expression in renal neoplasms: correlation with tumor type and grade. *Am J Clin Pathol* 134 (6): 873–879. DOI: 10.1309/AJCPPPR57HNJMSLZ .

47. Geyer RR, Zhao P, Parker MD, *et al* (2017) A Novel Stopped-Flow Assay for Quantitating Carbonic-Anhydrase Activity and Assessing Red-Blood-Cell Hemolysis. *Front Physiol* 28 (8):169. DOI: 10.3389/fphys.2017.00169 , PMCID: PMC5368281, PMID: 28400735.

48. Grüner B, Brynda J, Das V, Šícha V, Štěpánková J, Nekvinda J, *et al* (2019) Metallacarborane Sulfamides: Unconventional, Specific, and Highly Selective Inhibitors of Carbonic Anhydrase IX. *J Med Chem* 62 (21): 9560-9575. DOI: 10.1021/acs.jmedchem.9b00945 , PMID: 31568723.

49. Haapasalo J, Hilvo M, Nordfors K, *et al* (2008) Identification of an alternatively spliced isoform of carbonic anhydrase XII in diffusely infiltrating astrocytic gliomas. *Neuro Oncol* 10 (2): 131–138. DOI: 10.1215/15228517-2007-065 , PMID: 18322268.

50. Hilvo M, Baranauskiene L, Salzano AM, Scaloni A, Matulis D, *et al* (2008) Biochemical characterization of CA IX, one of the most active carbonic anhydrase isozymes. *J Biol Chem* 283 (410: 27799–27809. DOI: 10.1074/jbc.M800938200 , PMID: 18703501

51. Hirota J, Ando H, Hamada K, *et al* (2003) Carbonic anhydrase-related protein is a novel binding protein for inositol 1,4,5-trisphosphate receptor type 1. *Biochem J*. 372 (2): 435–441. DOI: 10.1042/BJ20030110 , PMCID: PMC1223404 , PMID: 12611586.

52. Hynninen P, Vaskivuo L, Saarnio J, *et al* (2006) Expression of transmembrane carbonic anhydrases IX and XII in ovarian tumours. *Histopathology* 49 (6): 594–602. DOI: 10.1111/j.1365-2559.2006.02523.x , PMID: 17163844.

53. Ilie M, Mazure NM, Hofman V, *et al* (2010) High levels of carbonic anhydrase IX in tumour tissue and plasma are biomarkers of poor prognostic in patients with non-small cell lung cancer. *Br J Cancer* 102 (11): 1627–1635. DOI: 10.1038/sj.bjc.6605690 , PMCID: PMC2883156 , PMID: 20461082.

54. Imtaiyaz Hassan M, Shajee B, Waheed A, Ahmad F, Sly WS (2012) Structure, function and applications of carbonic anhydrase isozymes. *Bioorg Med Chem* 15;21(6): 1570-1582. DOI: 10.1016/j.bmc.2012.04.044 , PMID: 22607884.

55. Innocenti A, Öztürk Sarıkaya SB, Gülçin I, Supuran CT (2010) Carbonic anhydrase inhibitors. Inhibition of mammalian isoforms I-XIV with a series of natural product polyphenols and phenolic acids. *Bioorg Med Chem* 18 (6): 2159–2164. DOI: 10.1016/j.bmc.2010.01.076 , PMID: 20185318.

56. Innocenti A, Scozzafava A, Parkkila S, *et al* (2008) Investigations of the esterase, phosphatase, and sulfatase activities of the cytosolic mammalian carbonic anhydrase isoforms I, II, and XIII with 4-nitrophenyl esters as substrates. *Bioorgan Med Chem Lett* 18 (7): 2267–2271. DOI: 10.1016/j.bmcl.2008.03.012 .

57. Innocenti A, Vullo D, Scozzafava A, Supuran CT (2008) Carbonic anhydrase inhibitors. Interactions of phenols with the 12 catalytically active mammalian isoforms (CA I–XIV). *Bioorg Med Chem Lett* 18 (5): 1583–1587. DOI: 10.1016/j.bmcl.2008.01.077 , PMID: 18242985.

58. Innocenti A, Vullo D, Scozzafava A, Supuran CT (2008) Carbonic anhydrase inhibitors. Inhibition of mammalian isoforms I–XIV with a series of substituted phenols including paracetamol and salicylic acid. *Bioorg Med Chem* 16: 7424–7428. DOI: 10.1016/j.bmc.2008.06.013 .

59. Ivaniz S, Liao SY, Ivaniz A, *et al* (2001) Expression of hypoxia-inducible cell-surface transmembrane carbonic anhydrases in human cancer. *Am J Pathol* 158 (3): 905–919. DOI: 10.1016/S0002-9440(10)64038-2

60. Jamali S, Klier M, Ames S, Barros LF, McKenna R, Deitmer JW, Becker HM (2015) Hypoxia-induced carbonic anhydrase IX facilitates lactate flux in human breast cancer cells by non-catalytic function. *Sci Rep* 5:13605. DOI: 10.1038/srep13605 .

61. Kardoush MI, Ward BJ, Ndao M (2017) Serum Carbonic Anhydrase 1 is a Biomarker for Diagnosis of Human Schistosoma mansoni Infection. *Am J Trop Med Hyg* 96(4): 842–849. DOI: 10.4269/ajtmh.16-0021 , PMCID: PMC5392630 , PMID: 28500821.

62. Karjalainen SL, Haapasalo HK, Aspatwar A, *et al* (2018) Carbonic anhydrase related protein expression in astrocytomas and oligodendroglial tumors. *BMC Cancer* 18 (1):584. DOI: 10.1186/s12885-018-4493-4 .

63. Kaunisto K, Parkkila S, Rajaniemi H, *et al* (2002) Carbonic anhydrase XIV: luminal expression suggests key role in renal acidification. *Kidney Int* 61 (6): 2111–2118. DOI: 10.1046/j.1523-1755.2002.00371.x , PMID: 12028451.

64. Khalifah RG (1971) Carbon dioxide hydration activity of carbonic anhydrase.1. Stop-flow kinetic studies on native human isoenzyme-b and isoenzyme-c. *J Biol Chem* 246 (8): 2561–2573. PMID: 4994926.

65. Kharbanda KK, Vigneswara V, McVicker BL, *et al* (2009) Proteomics reveal a concerted upregulation of methionine metabolic pathway enzymes, and downregulation of carbonic anhydrase-III, in betaine supplemented ethanol-fed rats. *Biochem Biophys Res Commun* 381(4): 523–527. DOI: 10.1016/j.bbrc.2009.02.082 , PMCID: PMC2670967 , PMID: 19239903.

66. Kim JY, Lee SH, An S, *et al* (2018) Carbonic anhydrase 9 expression in well-differentiated pancreatic neuroendocrine neoplasms might be associated with aggressive behavior and poor survival. *Virchows Arch* 472 (5): 739–748. DOI: 10.1007/s00428-018-2353-x , PMID: 29666945.

67. Kivela A, Parkkila S, Saarnio J, *et al* (2000) Expression of a novel transmembrane carbonic anhydrase isozyme XII in normal human gut and colorectal tumors. *Am J Pathol* 156 (2): 577–584. DOI: 10.1016/S0002-9440(10)64762-1 , PMID: 10666387.

68. Kivelä AJ, Kivelä J, Saarnio J, Parkkila S (2005_ Carbonic anhydrases in normal gastrointestinal tract and gastrointestinal tumours. *World J Gastroenterol* 11(2):155-163. doi: 10.3748/wjg.v11.i2.155. PMID: 15633208; PMCID: PMC4205394

69. Korkeila E, Talvinen K, Jaakkola PM, *et al* (2009) Expression of carbonic anhydrase IX suggests poor outcome in rectal cancer. *Br J Cancer* 100 (6): 874–880. DOI: 10.1038/sj.bjc.6604949 , PMID: 19240720.

70. Kovalevskiy O, Nicholls RA, Long F, Carlon A, Murshudov GN (2018) Overview of refinement procedures within REFMAC5: utilizing data from different sources. *Acta Crystallogr D Struct Biol* 74 (3): 215-227. doi: 10.1107/S2059798318000979. Epub 2018 Mar 2. PMID: 29533229; PMCID: PMC5947762.

71. Krall N, Pretto F, Mattarella M, *et al* (2016) A 99mTc-Labeled Ligand of Carbonic Anhydrase IX Selectively Targets Renal Cell Carcinoma In Vivo. *J Nucl Med* 57 (6): 943–949. DOI: 10.2967/jnumed.115.170514 , PMID: 26912427.

72. Krishnamurthy VM, Kaufman GK, Urbach AR, Gitlin I, Gudiksen KL, Weibel DB, Whitesides GM (2008) Carbonic anhydrase as a model for biophysical and physical-organic studies of proteins and protein-ligand binding. *Chem Rev* 108 (3): 946-1051. doi: 10.1021/cr050262p. PMID: 18335973; PMCID: PMC2740730.

73. Kugler M, Holub J, Brynda J, Pospíšilová K, Anwar SE, Bavol D, Havránek M, Král V, Fábry M, Grüner B, Řezáčová P (2020) The structural basis for the selectivity of sulfonamido dicarbaboranes toward cancer-associated carbonic anhydrase IX. *J Enzyme Inhib Med Chem* 35 (1): 1800-1810. doi: 10.1080/14756366.2020.1816996. PMID: 32962427; PMCID: PMC7534198

74. Kummola L, Hamalainen JM, Kivela J, *et al* (2005) Expression of a novel carbonic anhydrase, CA XIII, in normal and neoplastic colorectal mucosa. *BMC Cancer* 18;5:41. DOI: 10.1186/1471-2407-5-41 .

75. Kupriyanova E, Pronina N, Los D (2017) Carbonic anhydrase – a universal enzyme of the carbon-based life. *Photosynthetica* 55 (1): 3-19. DOI: 10.1007/s11099-017-0685-4.

76. Lakkis MM, Bergenhem NC, O'Shea KS, Tashian RE (1997) Expression of the acatalytic carbonic anhydrase VIII gene, Car8, during mouse embryonic development. *Histochem J* 29 (2): 135–141. DOI: 10.1023/a:1026433321974 , PMID: 9147070.

77. Lee M, Vecchio-Pagan B, Sharma N, *et al* (2016) Loss of carbonic anhydrase XII function in individuals with elevated sweat chloride concentration and pulmonary airway disease. *Hum Mol Genet* 25 (10): 1923–1933. DOI: 10.1093/hmg/ddw065 .

78. Lee S, Shin HJ, Han IO, *et al* (2007) Tumor carbonic anhydrase 9 expression is associated with the presence of lymph node metastases in uterine cervical cancer. *Cancer Sci* 98 (3): 329–333. DOI: 10.1111/j.1349-7006.2007.00396.x , PMID: 17233814 .

79. Lehtonen J, Shen B, Vihinen M, *et al* (2004) Characterization of CA XIII, a novel member of the carbonic anhydrase isozyme family. *J Biol Chem* 79 (4): 2719–2727. DOI: 10.1074/jbc.M308984200 , PMID: 14600151.

80. Liao SY, Ivanov S, Ivanova A, *et al* (2003) Expression of cell surface transmembrane carbonic anhydrase genes CA9 and CA12 in the human eye: overexpression of CA12 (CAXII) in glaucoma. *J Med Genet* 40 (4): 257–261. DOI: 10.1136/jmg.40.4.257 , PMCID: PMC1735430 , PMID: 12676895.

81. Lindskog S, Silverman DN (2000) The catalytic mechanism of mammalian carbonic anhydrases. *EXS* 2000 (90): 175-195. DOI: 10.1007/978-3-0348-8446-4_10 PMID: 11268516.

82. Long F, Nicholls RA, Emsley P, Graæulis S, Merkys A, Vaitkus A, Murshudov GN (2017) AceDRG: a stereochemical description generator for ligands. *Acta Crystallogr D*

Struct Biol 73 (2): 112-122. doi: 10.1107/S2059798317000067. Epub 2017 Feb 1. PMID: 28177307; PMCID: PMC5297914.

83. Lonnerholm G, Wistrand P (1983) Carbonic anhydrase in the human fetal gastrointestinal tract. *Biol Neonate* 44(3):166–176. DOI: 10.1159/000241711 .

84. Mahon BP, Bhatt A, Socorro L, Driscoll JM, Okoh C, Lomelino CL, Mboge MY, Kurian JJ, Tu C, Agbandje-McKenna M, *et al* (2016) The Structure of Carbonic Anhydrase IX Is Adapted for Low-pH Catalysis. *Biochemistry* 55: 4642–4653. DOI: 10.1021/acs.biochem.6b00243

85. Mahon P, Pinard MA, McKenna R (2015) Targeting Carbonic Anhydrase IX Activity and Expression. *Molecules* 20(2): 2323-2348. DOI: 10.3390/molecules20022323, PMCID: PMC6272707, PMID: 25647573.

86. Maleth J, Hegyi P (2014) Calcium signaling in pancreatic ductal epithelial cells: an old friend and a nasty enemy. *Cell Calcium* 55 (6): 337–345. DOI: 10.1016/j.ceca.2014.02.004 , PMID: 24602604.

87. Mallis RJ, Poland BW, Chatterjee TK, Fisher RA, Darmawan S, Honzatko RB, Thomas JA (2000) Crystal structure of S-glutathiolated carbonic anhydrase III. *FEBS Lett* 482 (3): 237-241. DOI: 10.1016/s0014-5793(00)02022-6 PMID: 11024467.

88. Maresca A, Akyuz G, Osman SM, *et al* (2015) Inhibition of mammalian carbonic anhydrase isoforms I-XIV with a series of phenolic acid esters. *Bioorg Med Chem* 23 (22): 7181–7188. DOI: 10.1016/j.bmc.2015.10.014 , PMID: 26498394.

89. Maresca A, Scozzafava A, Supuran CT (2010) 7,8-Disubstituted- but not 6,7-disubstituted coumarins selectively inhibit the transmembrane, tumor-associated carbonic anhydrase isoforms IX and XII over the cytosolic ones I and II in the low nanomolar/subnanomolar range. *Bioorg Med Chem Lett* 20 (24): 7255–7258. DOI: 10.1016/j.bmcl.2010.10.094 , PMID: 21067924.

90. Maresca A, Supuran CT (2010) Coumarins incorporating hydroxy- and chloromoieties selectively inhibit the transmembrane, tumor-associated carbonic anhydrase

isoforms IX and XII over the cytosolic ones I and II. *Bioorg Med Chem Lett* 20 (15): 4511–4514. DOI: 10.1016/j.bmcl.2010.06.040 , PMID: 20580555.

91. Maresca A, Temperini C, Pochet L, *et al* (2010) Deciphering the mechanism of carbonic anhydrase inhibition with coumarins and thiocoumarins. *J Med Chem* 53 (1): 335–344. DOI: 10.1021/jm901287j , PMID: 19911821.

92. Maresca A, Temperini C, Vu H, *et al* (2009) Non-zinc mediated inhibition of carbonic anhydrases: coumarins are a new class of suicide inhibitors. *J Am Chem Soc* 131 (8): 3057–3062. DOI: 10.1021/ja809683v , PMID: 19206230.

93. Martin D, Hann Z, Cohen S (2013) Metalloprotein–Inhibitor Binding: Human Carbonic Anhydrase II as a Model for Probing Metal–Ligand Interactions in a Metalloprotein Active Site. *Inorganic Chemistry* 52: 12207–12215. DOI: 10.1021/ic400295f .

94. Martin DP, Cohen SM (2012) Nucleophile recognition as an alternative inhibition mode for benzoic acid based carbonic anhydrase inhibitors. *Chem Commun (Camb)* 48 (43): 5259–5261. DOI: 10.1039/c2cc32013d , PMCID: PMC3674230, PMID: 22531842.

95. Maupin CM, Castillo N, Taraphder S, Tu C, McKenna R, Silverman DN, *et al* (2011) Chemical rescue of enzymes: proton transfer in mutants of human carbonic anhydrase II. *J Am Chem Soc* 133 (16): 6223–6234. DOI: 10.1021/ja1097594 , PMCID: PMC4120857 , PMID: 21452838.

96. Mikoshiba K, Okano H, Miyawaki A, *et al* (1995) Molecular genetic analyses of myelin deficiency and cerebellar ataxia. *Prog Brain Res* 105:23–41. DOI: 10.1016/S0079-6123(08)63281-1.

97. Minn I, Koo SM, Lee HS, *et al* (2016) [64Cu]XYIMSR-06: A dual-motif CAIX ligand for PET imaging of clear cell renal cell carcinoma. *Oncotarget* 7 (35): 56471–56479. DOI: 10.18632/oncotarget.10602 , PMCID: PMC5302928 , PMID: 27437764.

98. Mishra CB, Tiwari M & Supuran CT (2020) Progress in the development of human carbonic anhydrase inhibitors and their pharmacological applications: Where are we today? *Med Res Rev* 40 (6): 2485–2565. DOI: 10.1002/med.21713 , PMID: 32691504.

99. Mitterberger MC, Kim G, Rostek U, Levine RL, Zwerschke W (2012) Carbonic anhydrase III regulates peroxisome proliferator-activated receptor-γ2. *Exp Cell Res* 318 (8): 877–886. DOI: 10.1016/j.yexcr.2012.02.011 , PMCID: PMC3328775, PMID: 22507175.

100. Morgan PE, Pastorekova S, Stuart-Tilley A K, Alper SL, Casey JR (2007) Interactions of transmembrane carbonic anhydrase, CAIX, with bicarbonate transporters. *Am J Physiol Cell Physio* 293 (2): 738–748. DOI: 10.1152/ajpcell.00157.2007 .

101. Mori K, Ogawa Y, Ebihara K, *et al* (1999) Isolation and characterization of CA XIV, a novel membrane-bound carbonic anhydrase from mouse kidney. *J Biol Chem* 274 (22): 15701–15705. DOI: 10.1074/jbc.274.22.15701 .

102. Morimoto K, Nishimori I, Takeuchi T, *et al* (2005) Overexpression of carbonic anhydrase-related protein XI promotes proliferation and invasion of gastrointestinal stromal tumors. *Virchows Arch* 447 (1): 66–73. DOI: 10.1007/s00428-005-1225-3 , PMID: 15942747.

103. Morrisson JWM, Williams JF (1979) The kinetics of reversible tight-binding inhibition. *Methods Enzymol* 63:437–467. DOI: 10.1016/0076-6879(79)63019-7 .

104. Murshudov GN, Skubák P, Lebedev AA, Pannu NS, Steiner RA, Nicholls RA, Winn MD, Long F, Vagin AA (2011) REFMAC5 for the refinement of macromolecular crystal structures. *Acta Crystallogr D Biol Crystallogr* 67 (4): 355-367. doi: 10.1107/S0907444911001314. Epub 2011 Mar 18. PMID: 21460454; PMCID: PMC3069751.

105. Murshudov GN, Vagin AA, Dodson EJ (1997) Refinement of macromolecular structures by the maximum-likelihood method. *Acta Crystallogr D Biol Crystallogr* 53 (3): 240-255. DOI: 10.1107/S0907444996012255 , PMID: 15299926.

106. Nagao Y, Platero JS, Waheed A, *et al* (1993) Human mitochondrial carbonic anhydrase: cDNA cloning, expression, subcellular localization, and mapping to chromosome

16. *Proc Natl Acad Sci U S A* 90 (16): 7623–7627. DOI: 10.1073/pnas.90.16.7623 , PMCID: PMC47194 , PMID: 8356065.

107. Nagelhus EA, Mathiisen TM, Bateman AC, Haug FM, Ottersen OP, Grubb JH, *et al* (2005) Carbonic anhydrase XIV is enriched in specific membrane domains of retinal pigment epithelium, Muller cells, and astrocytes. *Proc Natl Acad Sci USA* 102 (22): 8030–8035. DOI: 10.1073/pnas.0503021102 , PMCID: PMC1142392, PMID: 15901897.

108. Nair SK, Christianson DW (1991) Structural properties of human carbonic anhydrase II at pH 9.5. *Biochem. Biophys. Res. Commun* 181 (2): 579-584. DOI: 10.1016/0006-291x(91)91229-6 , PMID: 1755840.

109. Nair SK, Ludwig PA, Christianson DW (1994) Two-site binding of phenol in the active site of human carbonic anhydrase II: structural implications for substrate association. *J Am Chem Soc* 116: 3659–3660. DOI: 10.1021/ja00087a086.

110. Nicholls RA, Tykac M, Kovalevskiy O, Murshudov GN (2018) Current approaches for the fitting and refinement of atomic models into cryo-EM maps using CCP-EM. *Acta Crystallogr D Struct Biol* 74 (6): 492-505. doi: 10.1107/S2059798318007313. Epub 2018 May 30. PMID: 29872001; PMCID: PMC6096485.

111. Nishikata M, Nishimori I, Taniuchi K, *et al* (2007) Carbonic anhydrase-related protein VIII promotes colon cancer cell growth. *Mol Carcinog* 46 (3): 208–214. DOI: 10.1002/mc.20264.

112. Nishimori I, Miyaji E, Morimoto K, *et al* (2005) Serum antibodies to carbonic anhydrase IV in patients with autoimmune pancreatitis. *Gut* 54 (2): 274–281. PMID: 15647194, PMCID: PMC1774835.

113. Ochi F, Shiozaki A, Ichikawa D, *et al* (2015) Carbonic Anhydrase XII as an Independent Prognostic Factor in Advanced Esophageal Squamous Cell Carcinoma. *J Cancer* 6 (10): 922–929. DOI: 10.7150/jca.11269 , PMCID: PMC4543752 , PMID: 26316888.

114. Opavsky R, Pastorekova S, Zelnik V, Gibadulinova A, Stanbridge EJ (1996) Human MN/CA9 gene, a novel member of the carbonic anhydrase family: structure and exon to

protein domain relationships. *Genomics* 33 (3): 480-487. DOI: 10.1006/geno.1996.0223 , PMID: 8661007.

115. Parkkila S, Parkkila AK, Saarnio J, *et al* (2000) Expression of the membrane-associated carbonic anhydrase isozyme XII in the human kidney and renal tumors. *J Histochem Cytochem* 48 (12):1601–1608. DOI: 10.1177/002215540004801203 , PMID: 11101628.

116. Pastorek J, Pastorekova S (2015) Hypoxia-induced carbonic anhydrase IX as a target for cancer therapy: from biology to clinical use. *Semin Cancer Biol* 31: 52–64. DOI: 10.1016/j.semcancer.2014.08.002 .

117. Pastorekova S, Gillies RJ (2019) The role of carbonic anhydrase IX in cancer development: links to hypoxia, acidosis, and beyond. *Cancer Metastasis Rev* 38 (1-2): 65–77. DOI: 10.1007/s10555-019-09799-0 , PMID: 31076951, PMCID: PMC6647366 .

118. Pastorekova S, Zavadova Z, Kostal M, Babusikova O, Zavada J, *et al* (1992) A novel quasi-viral agent, MaTu, is a two-component system. *Virology* 187 (2): 620-626. DOI: 10.1016/0042-6822(92)90464-z , PMID: 1312272.

119. Pertovaara M, Bootorabi F, Kuuslahti M, *et al* (2011) Novel carbonic anhydrase autoantibodies and renal manifestations in patients with primary Sjogren's syndrome. *Rheumatology (Oxford)* 50 (8): 1453–1457. DOI: 10.1093/rheumatology/ker118 , PMID: 21427176.

120. Pilka ES, Kochan G, Oppermann U, Yue WW (2012) Crystal structure of the secretory isozyme of mammalian carbonic anhydrases CA VI: implications for biological assembly and inhibitor development. *Biochem Biophys Res Commun* 419 (3): 485–489. DOI: 10.1016/j.bbrc.2012.02.038 , PMID: 22366092.

121. Pinard MA, Boone CD, Rife BD, Supuran CT, McKenna R (2013) Structural study of interaction between brinzolamide and dorzolamide inhibition of human carbonic anhydrases. *Bioorg Med Chem* 21 (22): 7210-7215. DOI: 10.1016/j.bmc.2013.08.033 , PMID: 24090602.

122. Power KA, Grad S, Rutges JP, *et al* (2011) Identification of cell surface-specific markers to target human nucleus pulposus cells: expression of carbonic anhydrase XII varies with age and degeneration. *Arthritis Rheum* 63 (12): 3876–3886. DOI: 10.1002/art.30607 .

123. Proescholdt MA, Mayer C, Kubitza M, *et al* (2005) Expression of hypoxia-inducible carbonic anhydrases in brain tumors. *Neuro Oncol* 7 (4): 465–475. DOI: 10.1215/S1152851705000025.

124. Riafrecha LE, Rodríguez OM, Vullo D, *et al* (2013) Synthesis of C-cinnamoyl glycosides and their inhibitory activity against mammalian carbonic anhydrases. *Bioorg Med Chem* 21 (6): 1489–1494. DOI: 10.1016/j.bmc.2012.09.002 , PMID: 23010455.

125. Richardson SM, Ludwinski FE, Gnanalingham KK, *et al* (2017) Notochordal and nucleus pulposus marker expression is maintained by sub-populations of adult human nucleus pulposus cells through aging and degeneration. *Sci Rep* 7 (1):1501. DOI: 10.1038/s41598-017-01567-w .

126. Ruusuvuori E, Huebner AK, Kirilkin I, *et al* (2013) Neuronal carbonic anhydrase VII provides GABAergic excitatory drive to exacerbate febrile seizures. *EMBO J* 32 (16): 2275–2286. DOI: 10.1038/emboj.2013.160.

127. Saarnio J, Parkkila S, Parkkila AK, *et al* (1998) Immunohistochemical study of colorectal tumors for expression of a novel transmembrane carbonic anhydrase, MN/CA IX, with potential value as a marker of cell proliferation. *Am J Pathol* 153 (1): 279–285. DOI: 10.1016/S0002-9440(10)65569-1 , PMID: 9665489.

128. Sahin H, Can Z, Yildiz O, *et al* (2012) Inhibition of carbonic anhydrase isozymes I and II with natural products extracted from plants, mushrooms and honey. *J Enzyme Inhib Med Chem* 27 (3): 395–402. DOI: 10.3109/14756366.2011.593176 , PMID: 21740099.

129. Saito R, Watanabe H, Asano T, *et al* (2013) Anti-carbonic anhydrase III autoantibodies in vasculitis syndrome. *Int J Rheum Dis* 16 (3): 339–46. DOI: 10.1111/1756-185X.12089 , PMID: 23981757.

130. Sawicki M, Sypniewska G, Krintus M, *et al* (2008) Multi-Marker Approach with the Use of Biochip Cardiac Array Technology for Early Diagnosis in Patients with Acute Coronary Syndromes. *EJIFCC* 19(3):160–171. PMCID: PMC4975262 , PMID: 27683314.

131. Scozzafava A, Menabuoni L, Mincione F, *et al* (1999) Carbonic anhydrase inhibitors. Synthesis of water-soluble, topically effective, intraocular pressure-lowering aromatic/heterocyclic sulfonamides containing cationic or anionic moieties: is the tail more important than the ring? *J Med Chem* 42 (14): 2641–2650 DOI: 10.1021/jm9900523 , PMID: 10411484.

132. Scozzafava A, Menabuoni L, Mincione F, Supuran CT (2002) Carbonic anhydrase inhibitors. A general approach for the preparation of water-soluble sulfonamides incorporating polyamino-polycarboxylate tails and of their metal complexes possessing long-lasting, topical intraocular pressure-lowering properties. *J MedChem* 45 (7): 1466–1476. DOI: 10.1021/jm0108202 , PMID: 11906288.

133. Şentürk M, Gülçin I, Daştan A, *et al* (2009) Carbonic anhydrase inhibitors. Inhibition of human erythrocyte isozymes I and II with a series of antioxidant phenols. *Bioorg Med Chem* 17 (8): 3207–3211. DOI: 10.1016/j.bmc.2009.01.067 , PMID: 19231207.

134. Shah GN, Hewett-Emmett D, Grubb JH, *et al* (2000) Mitochondrial carbonic anhydrase CA VB: differences in tissue distribution and pattern of evolution from those of CA VA suggest distinct physiological roles. *Proc Natl Acad Sci U S A* 97 (4): 1677–1682. DOI: 10.1073/pnas.97.4.1677 , PMCID: PMC26495 , PMID: 10677517.

135. Sharma A, Tiwari M, Supuran CT (2014) Novel coumarins and benzocoumarins acting as isoform-selective inhibitors against the tumor-associated carbonic anhydrase IX. *J Enzyme Inhib Med Chem* 29 (2): 292–296. DOI: 10.3109/14756366.2013.777334 , PMID: 23488741.

136. Shimahara H, Yoshida T, Shibata Y, Shimizu M, Kyogoku Y, Sakiyama F, *et al (2007)* Tautomerism of histidine 64 associated with proton transfer in catalysis of carbonic anhydrase. *J Biol Chem* 282 (13): 9646–9656. DOI: 10.1074/jbc.M609679200 , PMID: 17202139.

137. Simone GD, Supuran CT (2010) Carbonic anhydrase IX: Biochemical and crystallographic characterization of a novel antitumor target. *Biochimica et Biophysica Acta* 1804 (2): 404-409. DOI: 10.1016/j.bbapap.2009.07.027 , PMID: 19679200.

138. Sippel KH, Robbins AH, Domsic J, Genis C, Agbandje-McKenna M, McKenna R (2009) High-resolution structure of human carbonic anhydrase II complexed with acetazolamide reveals insights into inhibitor drug design. *Acta Crystallogr Sect F Struct Biol Cryst Commun* 65 (10): 992-995. doi: 10.1107/S1744309109036665. Epub 2009 Sep 25. PMID: 19851004; PMCID: PMC2765883.

139. Stadie WC, O'Brien H (1933) The catalysis of the hydration of carbon dioxide and the dehydration of carbonic acid by an enzyme isolated from red blood cells. *J Biol Chem* 103: 521–529. DOI: 10.1016/S0021-9258(18)75831-6.

140. Sun MK, Alkon DL (2002) Carbonic anhydrase gating of attention: memory therapy and enhancement. *Trends Pharmacol Sci* 23 (2): 83–89. DOI: 10.1016/s0165-6147(02)01899-0 .

141. Supuran C T (2015) How many carbonic anhydrase inhibition mechanisms exist? J *Enzyme Inhib Med Chem* 31(3): 345–360. DOI 10.3109/14756366.2015.1122001 , PMID: 26619898.

142. Supuran CT (2008) Carbonic anhydrases–an overview. *Curr Pharm Des* 14 (7): 603–614. DOI: 10.2174/138161208783877884 , PMID: 18336305.

143. Supuran CT (2011) Carbonic anhydrase inhibition with natural products: novel chemotypes and inhibition mechanisms. *Mol Divers* 15 (2): 305–316. DOI: 10.1007/s11030-010-9271-4 , PMID: 20803169.

144. Supuran CT (2016) Structure and function of carbonic anhydrases. *J Biochem* 473: 2023–2032. DOI: 10.1042/BCJ20160115 , PMID: 27407171.

145. Supuran CT, Scozzafava A, Casini A. (2003) Carbonic anhydrase inhibitors. *Med Res Rev* 23 (2): 146-89. DOI: 10.1002/med.10025, PMID: 12500287.

146. Svastová E, Hulíková A , Rafajová M, Zat'ovicová M, Gibadulinová A, *et al* (2004). Hypoxia activates the capacity of tumor-associated carbonic anhydrase IX to acidify extracellular pH. *FEBS Letters* 577(3): 439–445. DOI: 10.1016/j.febslet.2004.10.043 , PMID: 15556624.

147. Svastova E, Witarski W, Csaderova L, Kosik I, Skvarkova L, Hulikova A, Zatovicova M, Barathova M, Kopacek J, Pastorek J, Pastorekova S (2012) Carbonic anhydrase IX interacts with bicarbonate transporters in lamellipodia and increases cell migration via its catalytic domain. *J Biol Chem* 287 (5): 3392–3402. DOI: 10.1074/jbc.M111.286062 .

148. Takakura M, Yokomizo A, Tanaka Y, *et al* (2012) Carbonic anhydrase I as a new plasma biomarker for prostate cancer. *ISRN Oncol* 2012:768190. DOI: 10.5402/2012/768190, PMCID: PMC3506895, PMID: 23213568.

149. Taniuchi K, Nishimori I, Takeuchi T, *et al* (2002) Developmental expression of carbonic anhydrase-related proteins VIII, X, and XI in the human brain. *Neuroscience* 112 (1): 93–99. DOI: 10.1016/s0306-4522(02)00066-0 , PMID: 12044474.

150. Tars K, Vullo D, Kazaks A, *et al* (2013) Sulfocoumarins (1,2-benzoxathiine-2,2-dioxides): a class of potent and isoform-selective inhibitors of tumor-associated carbonic anhydrases. *J Med Chem* 56 (1): 293–300. DOI: 10.1021/jm301625s , PMID: 23241068.

151. Touisni N, Maresca A, McDonald PC, *et al* (2011) Glycosyl coumarin carbonic anhydrase IX and XII inhibitors strongly attenuate the growth of primary breast tumors. *J Med Chem* 54 (24): 8271–8277. DOI: 10.1021/jm200983e , PMID: 22077347.

152. Tureci O, Sahin U, Vollmar E, *et al* (1998) Human carbonic anhydrase XII: cDNA cloning, expression, and chromosomal localization of a carbonic anhydrase gene that is

overexpressed in some renal cell cancers. *Proc Natl Acad Sci U S A* 95 (13): 7608–7613. DOI: 10.1073/pnas.95.13.7608 .

153. van Karnebeek CD, Sly WS, Ross CJ, *et al* (2014) Mitochondrial carbonic anhydrase VA deficiency resulting from CA5A alterations presents with hyperammonemia in early childhood. *Am J Hum Genet* 94 (3): 453–461. DOI: 10.1016/j.ajhg.2014.01.006 , PMCID: PMC3951944 , PMID: 24530203.

154. Watson PH, Chia SK, Wykoff CC, *et al* (2003) Carbonic anhydrase XII is a marker of good prognosis in invasive breast carcinoma. *British Journal Of Cancer* 88 (7):1065-1070. DOI: 10.1038/sj.bjc.6600796.

155. Wykoff CC, Beasley NJ, Watson PH, Turner KJ, Pastorek J, *et al* (2000) Hypoxia-inducible expression of tumor-associated carbonic anhydrases. *Cancer Res*. 60 (24): 7075–7083. PMID: 11156414.

156. Yoo CW, Nam BH, Kim JY, *et al* (2010) Carbonic anhydrase XII expression is associated with histologic grade of cervical cancer and superior radiotherapy outcome. *Radiat Oncol* 1;5:101. DOI: 10.1186/1748-717X-5-101 , PMCID: PMC2990746 , PMID: 21040567.

157. Yung-Chi C, Prusoff WH (1973) Relationship between the inhibition constant (Ki) and the concentration of inhibitor which causes 50 per cent inhibition (I50) of an enzymatic reaction. *Biochem Pharmacol* 22 (23): 3099–3108. DOI: 10.1016/0006-2952(73)90196-2 , PMID: 4202581.

158. Zamanova S, Shabana AM, Mondal UK, Ilies MA (2019) Carbonic anhydrases as disease markers. *Expert Opin Ther Pat* 29 (7): 509-533. dOI: 10.1080/13543776.2019.1629419 , PMID: 31172829.

159. Zavada J, Zavadova Z, Pastorek J, *et al* (2000) Human tumour-associated cell adhesion protein MN/CA IX: identification of M75 epitope and of the region mediating cell adhesion. *Br J Cancer* 82 (11):1808–1813. DOI: 10.1054/bjoc.2000.1111 , PMCID: PMC2363230, PMID: 10839295.

160. Zavada J, Zavadova Z, Pastorekova S, Ciampor F, Pastorek J, *et al* (1993) Expression of MaTu-MN protein in human tumor cultures and in clinical specimens. *Int. J. Cancer* 54 (2): 268-274. DOI: 10.1002/ijc.2910540218 , PMID: 8486430.

161. https://www.biorender.com/

162. https://www.acdlabs.com/products/chemsketch/